#5 of 8

FINAL REPORT

AF19(604)-7400, Subcontract No. 251

THE ROTATING FIELD PHASER

The work reported in this document was performed under subcontract to Lincoln Laboratory, a center for research operated by Massachusetts Institute of Technology with the support of the United States Air Force under Contract AF 19(604)7400

Prepared for

Lincoln Laboratory
Lexington, Massachusetts

by

Hyletronics Corporation
185 Cambridge Street
Burlington, Massachusetts

Principal Investigator:
Dr. Jerald A. Weiss

Contents

Contents

Figures

1. Scope of the report.

This report presents the results of an investigation directed toward the development of a rotating-field phaser* utilizing the microwave properties of ferrite. The objective of the program was to advance the art of phaser design so as to extend the range of application of the device and to overcome some of the limitations inherent in existing devices which use other principles to perform the same circuit function.

In Sec. 2 the historical background of this work is summarized. Activity on the rather specialized problems associated with this type of magnetically actuated phaser has remained in the hands of a small number of workers over many years, and the results up to the present have been more in the nature of discussion and experimental illustration of the basic principles rather than the development of devices having direct practical application to microwave systems. As is usually the case in the early exploration of a novel device concept, the reasons for this relatively leisurely beginning are, first, that the exploratory work reveals certain limitations and problems whose magnitude is difficult to assess without a considerable amount of systematic study, and second, that the need for the particular combination of characteristics

*The term phaser will be used in this report to denote any transmission line device which provides variable electrical length while maintaining low and, ideally, constant insertion loss.

demonstrably or potentially available from the device in question has not yet been fully developed. The progress represented by the present work reflects the further evolution of this process: the incorporation of new and independent ideas has improved the outlook for practical realization of the device and has benefited from the emergence of more urgent and more specific system requirements.

In Sec. 3 the objectives of the present program are discussed, with emphasis on the concepts of dielectric-waveguide propagation and low-field differential phase effects. The exploratory part of the program was directed primarily toward the study of these effects as means for improving the suitability of the rotating-field phaser for system applications.

Sec. 4 presents an outline of the principles of operation, beginning with the elementary and idealized circuit-theory considerations of the continuously-variable rotating half-wave plate phaser and proceeding to the use of the gyromagnetic properties of ferrites as a means for achieving electronic phase control. The incorporation of dielectric-waveguide characteristics with the object of removing limitations in speed, bandwidth, and insertion loss is discussed.

In Sec. 5 the circuit theory is extended to include an analysis of the scattering due to mismatches and faulty conversion from circular to linear polarization. The need for this additional formulation arises from our experimental observation of the scattering effects which limit bandwidth

and distort the phase variation. Although these disturbing effects are still present in our most recent data, it is very encouraging to note that they display a degree of regularity which permits them to be diagnosed, correlated with measurable characteristics of the various components, and ultimately eliminated.

Sec. 6 contains a review of the experimental data, showing our most significant results at X-band on phase, insertion loss, and VSWR. The frequency-dependence of insertion loss is illustrated and discussed. Problems of magnetic control field requirement, hysteresis, temperature dependence, and the question of adapting the design for operation at other frequencies are considered. In Sec. 7 the experimental methods used to obtain these data are described. Sec. 8 presents a summary of our conclusions and prospects for further developments in rotating-field phaser design.

2. Background.

The concept of a continuously variable phaser employing a rotating half-wave section was introduced by A.G. Fox[1] in 1947. Fox considered a two-mode transmission line, such as circular waveguide, supporting a wave circularly-polarized in, say, the clockwise sense, incident on the input end. In traversing the half-wave element the wave is decomposed into two linearly-polarized normal modes, one of which is retarded one half-wavelength with respect to the other, so that the emerging wave is polarized in the opposite, counterclockwise, sense. He showed that the phase of the transmitted wave contains a variable part which is just equal to twice the angle of orientation ϑ of the principal axes of the half-wave plate with respect to a fixed set of reference axes. To construct a complete phase-shifter operating in single-mode guide, it is only necessary to add quarter-wave transducers at the input and output ends, to generate the required circular polarization and to convert it back to linear. The simplest embodiment of the principle is a circular waveguide containing suitably matched dielectric sheets of the proper lengths for the sequence of quarter-, half-, and quarter-wave sections, with mechanical facilities for rotating the half-wave section about its axis. Commercial devices of this kind are available. They are attractive for laboratory and test system use because of their considerable bandwidth, simple and precise calibration, and the feature of capitalizing on the multiple-valuedness of phase

- -

1. Literature references will be found on page 66.

angle for c-w signals so as to permit the phase to be advanced or retarded endlessly by a continuous rotation in one direction. This last characteristic has led to the application of the device as a single-sideband generator[2].

For radar, communications, and other more stringent system applications an electronically controllable, nonmechanical method of performing the same function would be extremely valuable. In 1952, (M.T.) Weiss and Fox[3] demonstrated birefringence produced by applying a d-c magnetic field in a transverse direction to a rod of ferrite mounted on the axis of circular waveguide. The gyromagnetic anisotropy of the ferrite provided the mechanism for removing the degeneracy of the circular guide and producing a phase differential between the normal modes of propagation, namely waves linearly polarized parallel and perpendicular to the direction of the applied field. This effect was also studied by Cacheris[4] in 1954, who used it to build a prototype version of a single-sideband generator in which the ferrite-loaded circular guide acted as a half-wave plate, driven by a rotating magnetic field at a modulation frequency of 20 Kc. The device was designed for X-band; it operated best over a 100 Mc band at 9300 Mc, yielding about 1 db insertion loss, with suppression of the carrier and undesired sideband signals to 30 and 45 db, respectively.

In 1956 Karayianis and Cacheris[5] continued the study of ferrite differential-phase effects in an effort to obtain optimum broadband characteristics and to reduce the d-c magnetic

field requirement. Their best results were for the case of a ferrite tube lining the wall of a reduced-diameter circular guide: the field was 210 oersteds and the insertion loss fluctuated between about 1.5 and 3 db over the band from 9.0 to 9.7 KMc.

3. Objectives of the program.

The present investigation also involved the use of a ferrite tube as the differential-phase element, but was conceived independently and directed toward different and more ambitious objectives. The goal of producing high-speed phase changes for applications such as phase-controlled antenna arrays and single-sideband generation demands that the main factors limiting speed, namely the large magnitude of the magnetic control field and the intervention of a conductive waveguide wall between the external electromagnet and the active ferrite element, be eliminated. The use of a tube of the proper dimensions offers the possibility of removing these limitations while preserving the valuable characteristics of the device, particularly broad operating band and continuous variability.

The dielectric constant of microwave ferrites is in the range 9 to 13, and that of the ferromagnetic garnets somewhat higher, about 15. By proper selection of dimensions a ferrite rod or tube may be made to act as a dielectric waveguide propagating in the "dipole" (HE_{11}) mode which possesses the same symmetry as the dominant TE_{11} mode in circular guide. The characteristics of this mode have been discussed by Elsasser[6] and others. Applications of dielectric waveguide effects to ferrite devices[7] have led to important improvements in performance. The significant property of this type of propagation for magnetically variable devices is the fact that no conductive waveguide is required, the wave remaining tightly bound to the

interior and surface of the dielectric element. Thus the difficulties associated with the induction of eddy currents in the conducting wall of conventional-waveguide devices when the externally applied magnetic control field is changed do not arise here.

A solid rod of ferrite of the proper diameter can be made to present a good match to the dominant conductive-waveguide mode by the addition of dielectric transducers or tapers, and to support the desired dielectric-waveguide mode with low dissipative and radiative losses. There is some advantage in insertion loss and bandwidth if the ferrite element is made in the form of a tube[8], but these, while significant, are not the primary reason for our interest in the tube geometry in the present program. Rather, it was our expectation that the tube would offer a means for operating the device at exceptionally low d-c fields. Our efforts on this aspect of the investigation have not resulted in the desired low-field performance; however, neither have they excluded the possibility that further refinements in the design will lead to the improvement as originally envisioned.

A long ferromagnetic rod of circular cross-section, placed in a uniform d-c magnetic field with its axis transverse to the direction of the field, becomes uniformly magnetized. In this case the anisotropy leading to differential phase effects arises from the gyromagnetic interaction of the material with the r-f magnetic field of the wave, as demonstrated by Weiss and Fox[3] and by Cacheris[4]. As these authors

have shown, an estimate of the conditions required and of the magnitude of the effect may be obtained from the formulation by Polder[9] analyzing the interaction of a plane wave with a gyromagnetic medium. The magnitude of the d-c field required for appreciable effects is below that at which ferromagnetic resonance occurs, but is nevertheless associated with the resonance phenomenon; at X-band it is in the range of hundreds of oersteds.

If the ferrite rod is replaced by a circularly-cylindrical tube, the internal field within the material is no longer uniform. In the range of low applied fields where the ferrite is only partially magnetized this non-uniform field gives rise to a highly non-uniform state of magnetization having the required symmetry for differential phase effects. With proper selection of the ferrite composition and of the cross-sectional dimensions of the tube, it is possible to create an azimuthal variation in the r-f permeability which gives rise to the required differential phase effect. Further discussion of this mechanism is presented in Sec. 4.

The low-field variation in magnetization contemplated here is known to be applicable in practical microwave ferrite devices; the Reggia-Spencer phase shifter which depends on this mechanism for its operation has received experimental[10] and theoretical[11] attention and has been produced commercially. Although application of the effect to the rotating-field phaser depends on the achievement of a rather intricate combination of conditions, we believe that it can be done and that the result-

ing improvement in the device, namely reduction in magnetic control field requirement -- hence reduced size, weight, and control power, and improved speed -- will lead to a wide range of important system applications.

The objectives of the present program were to construct a prototype model of the rotating-field phaser for laboratory investigation and study it to determine the feasibility of the device for a phased array radar system. The primary activity, study of the structural details required to produce differential phase action in ferrite dielectric-waveguide at low fields, was to be performed at X-band, and the special problem of ferrite compositions suitable for use at L-band was to be investigated. Other characteristics of the unit which are of importance in system applications were to be studied; they were: insertion loss, linearity of phase shift with rotation of magnetic field, temperature dependence, hysteresis effects, and drive circuit requirements.

4. Principles of operation.

4A. Theory of phaser action.

With extensive experimental measurement and exploration as a background, we seek a model which contains the significant parameters controlling the scattering amplitudes and phases of the transversely-magnetized ferrite element together with its associated polarization transducers. As an introduction to the concepts and notation, we first analyze the structure under the simplest assumptions, namely that its components are uniform, lossless, and matched.

Consider a waveguide which supports two normal modes of propagation. We may regard the symmetry of the guide cross-section as elliptical and the normal modes as associated with linear polarizations in the directions of the principal axes, denoted by p and s. The complex amplitudes E_p and E_s at point z on the guide axis are given by

$$\begin{bmatrix} E_p(z) \\ E_s(z) \end{bmatrix} = \begin{bmatrix} e^{-i\beta_p z} & \\ & e^{-i\beta_s z} \end{bmatrix} \begin{bmatrix} E_p(0) \\ E_s(0) \end{bmatrix} \qquad (1)$$

The principal axes are oriented at the angle ϑ with respect to the "laboratory" axes x, y defined by the orientation of the single-mode rectangular guides at the input and output ends. Transforming to laboratory axes, we obtain

$$\begin{bmatrix} E_x(z) \\ E_y(z) \end{bmatrix} = \begin{bmatrix} e^{-i\beta_p z}\cos^2\vartheta + e^{-i\beta_s z}\sin^2\vartheta & (e^{-i\beta_p z} - e^{-i\beta_s z})\cos\vartheta\sin\vartheta \\ (e^{-i\beta_p z} - e^{-i\beta_s z})\cos\vartheta\sin\vartheta & e^{-i\beta_p z}\sin^2\vartheta + e^{-i\beta_s z}\cos^2\vartheta \end{bmatrix} \begin{bmatrix} E_x(0) \\ E_y(0) \end{bmatrix} \qquad (2)$$

Let $\beta_p = \beta+\delta$, $\beta_s = \beta-\delta$

Then the matrix of equation (2), which we shall denote by T, takes the form

$$T(2\delta z, \vartheta) = e^{-i\beta z} \times$$

$$\times \begin{bmatrix} \cos \delta z - i \sin \delta z \cos 2\vartheta & -i \sin \delta z \sin 2\vartheta \\ -i \sin \delta z \sin 2\vartheta & \cos \delta z + i \sin \delta z \cos 2\vartheta \end{bmatrix} \quad (3)$$

For the case of the ferrite section the principal axes p,s may be identified with the directions parallel and perpendicular, respectively, to the externally applied d-c magnetic field. The magnitude of the field is adjusted to produce the phase differential $2\delta z = \pi$ between the two normal modes in the length $z = \ell$. In this case,

$$T(\pi, \vartheta) = -ie^{-i\beta\ell} \begin{bmatrix} \cos 2\vartheta & \sin 2\vartheta \\ \sin 2\vartheta & -\cos 2\vartheta \end{bmatrix} \quad (4)$$

The matrix T of equation (3) also contains the case of a quarter-wave transducer, for which the electrical differential length is $2\delta z = \pi/2$ and the principal axes are oriented at $\vartheta = \pi/4$:

$$T(\pi/2, \pi/4) = \frac{1}{\sqrt{2}} e^{-i\beta\ell} \begin{bmatrix} 1 & -i \\ -i & 1 \end{bmatrix} \quad (5)$$

The average electrical length $\beta\ell$ need not, of course, be the same for the quarter-wave plate of (5) as it is for the half-wave plate of (4).

To illustrate the operation of the rotating field

phaser under ideal conditions, we consider the rotating half-wave section of (4) with quarter-wave transducers (5) at both ends:

$$T(\pi/2,\pi/4)T(\pi,\vartheta)T(\pi/2,\pi/4) = -ie^{-i\beta L}\begin{bmatrix} e^{-2i\vartheta} & \\ & -e^{2i\vartheta} \end{bmatrix} \qquad (6)$$

where βL denotes the electrical length of the combination as measured by the average propagation constant β. For a signal incident on the unit, polarized in the x direction, the total phase change in transmission is composed of the fixed part $-ie^{-i\beta L}$ together with the continuously variable part $e^{-2i\vartheta}$.

Equation (6) exhibits the basic function of the device; namely a matched transmission-line unit giving full transmission with phase precisely proportional to the angle of orientation of the magnetic control field.

4B. Propagation in a gyromagnetic medium.

As in the investigations of previous workers[3,4], the gyromagnetic property of ferrite which can serve to generate the differential phase effect described by equation (1) may be analyzed in an approximate way by applying the results of Polder[9] for the propagation of a plane wave through a lossless gyromagnetic medium defined by the permeability tensor

$$\underline{\underline{\mu}} = \begin{bmatrix} \mu & -i\kappa & \\ i\kappa & \mu & \\ & & 1 \end{bmatrix} \qquad (7)$$

where μ and K are related to the magnetization $4\pi M$, the d-c field H (assumed to be applied in the z-direction) and frequency ω by

$$\mu = 1 + \frac{4\pi\gamma^2 MH}{\gamma^2 H^2 - \omega^2} \quad , \quad K = \frac{4\pi\gamma M\omega}{\gamma^2 H^2 - \omega^2} \tag{8}$$

in which γ is the gyromagnetic ratio, $\gamma/2\pi = 2.8$ Mc per oersted. For the case of a wave propagating in a direction transverse to that of the d-c field, the effective permeability controlling the phase velocity depends on the polarization: μ_p and μ_s for waves having their r-f magnetic fields polarized respectively parallel and perpendicular to the z-direction are given by

$$\mu_p = 1 \quad , \quad \mu_s = 1 + \frac{4\pi\gamma^2 MB}{\gamma^2 BH - \omega^2} \tag{9}$$

where B is the induction $B = H + 4\pi M$. The phase differential $\Delta\varphi$ for propagation of the two types of waves over a distance l is then

$$\Delta\varphi = (\beta_p - \beta_s)l = 2\delta l = \frac{\omega l}{c}\sqrt{\epsilon}\,(\sqrt{\mu_p} - \sqrt{\mu_s}) \tag{10}$$

where ϵ is the dielectric constant of the medium and c is the velocity of light. For values of H appreciably less than that satisfying the resonance condition $\gamma^2 BH = \omega^2$ the phase difference is approximately

$$\Delta\varphi \cong \frac{2\pi l \gamma^2 MB\sqrt{\epsilon}}{\omega c} \tag{11}$$

To illustrate the meaning of this result, we may suppose that the saturation magnetization $4\pi M$ of the ferrite is in the

neighborhood of ω/γ and that H is much smaller than $4\pi M$. Then

$$\Delta\varphi \cong \frac{\omega l}{2c}\sqrt{\epsilon} \qquad (12)$$

Thus, under the idealized conditions considered, the phase differential between waves in the two polarizations would be of the same order of magnitude as the phase for propagation of a single plane wave in a dielectric medium characterized by ϵ.

Conditions resembling those contemplated in the above plane-wave approximation may be obtained by using a ferrite specimen in the form of a rod, provided the diameter of the rod is large enough to support most of the r-f energy. When such a large rod is used in conductive waveguide, however, it excites propagation in a number of spurious modes, causing undesirable fluctuations in insertion loss and phase. Another difficulty is that a strong magnetic field must be applied externally to overcome the demagnetizing effect of the surface of the rod.

Although equation (12) predicts an appreciable phase differential even when the internal d-c field is far below the resonance value, nevertheless the experience of Cacheris[4,5] and that of the present investigation is that fields of inconveniently large magnitudes are required in order to produce appreciable effects. This is due in part to the fact that a field equal to more than half the saturation magnetization $4\pi M_s$ must be applied to saturate the material when it is in the form of a rod with the field transverse to its axis. For

work at X-band, $4\pi M_s$ is usually in the range from 2000 to 3000 gauss (the single-sideband modulator of Cacheris[4] employed a material having $4\pi M_s \sim 3000$ gauss; in the present investigation values of $4\pi M_s$ from 1900 to 2400 gauss were used). Hence the internal fields have been small and the magnetization far below its saturation value. In the earlier and present work, improved phase differentials were observed when the rods were replaced by tubes. This was due primarily to the more favorable demagnetizing conditions, as analyzed in the following paragraph 4C.

4C. Magnetostatics of a tube.

The substitution of a tube in place of a rod of ferrite as the rotatable half-wave section serves several functions. First, the demagnetization is changed in such a way that in parts of the tube wall the applied d-c control field penetrates into the material more effectively; this enhances the magnitude of the internal d-c field. Second, there is a marked variation of the demagnetizing effect as a function of azimuth, or in other words a strongly inhomogeneous internal field; with the proper selection of ferrite composition such that the isotropic r-f permeability is dependent on the magnitude of the field, the net result is a highly anisotropic permeability having the correct symmetry to produce birefringence, leading to the desired phase differential. Third, the tube geometry has been shown[8] to possess potentially exceptional bandwidth, in the sense that dispersive effects

(frequency-dependence of wavelength, loss, and r-f field configuration) may be suppressed over a considerable frequency range when the inner and outer radii are properly selected in relation to the dielectric constant of the material.

The following analysis of the magnetostatic field yields the radial and azimuthal dependence of internal d-c field and magnetization as functions of the ratio ρ_o of inner to outer radius. Consider the tube illustrated in Fig. 1. We make the simplifying assumptions that end effects can be neglected, that the externally applied field H_o is uniform, and that the permeability μ of the material is independent of field; i.e., that the magnetization $4\pi\underline{M}$ is a linear function of field $\underline{H}$. Let $V(r, \vartheta)$ denote the magnetostatic potential; V satisfies

$$\nabla^2 V = \frac{1}{r}\frac{\partial}{\partial r}\left(r\frac{\partial V}{\partial r}\right) + \frac{1}{r^2}\frac{\partial^2 V}{\partial \vartheta^2} = 0 \qquad (13)$$

then $$V = \sum a_n V_n \ , \quad V_n = r^n \cos n\vartheta \ , \quad n = 0, \pm 1, \pm 2, \ldots \qquad (14)$$

For the case of a uniform field H_o applied in the direction $\vartheta = \pi$ we take $n = \pm 1$:

$$V = \left(a_1 r + \frac{a_{-1}}{r}\right)\cos\vartheta \qquad (15)$$

The boundary conditions are: V is finite at $r = 0$; V reduces to $V_o = H_o r \cos\vartheta$ as $r \to \infty$; $\mu H_r = -\mu \partial V/\partial r$ and $H_\vartheta = -(1/r)\partial V/\partial \vartheta$ are continuous at the inner and outer boundaries of the tube wall. These yield the required set of equations whose solu-

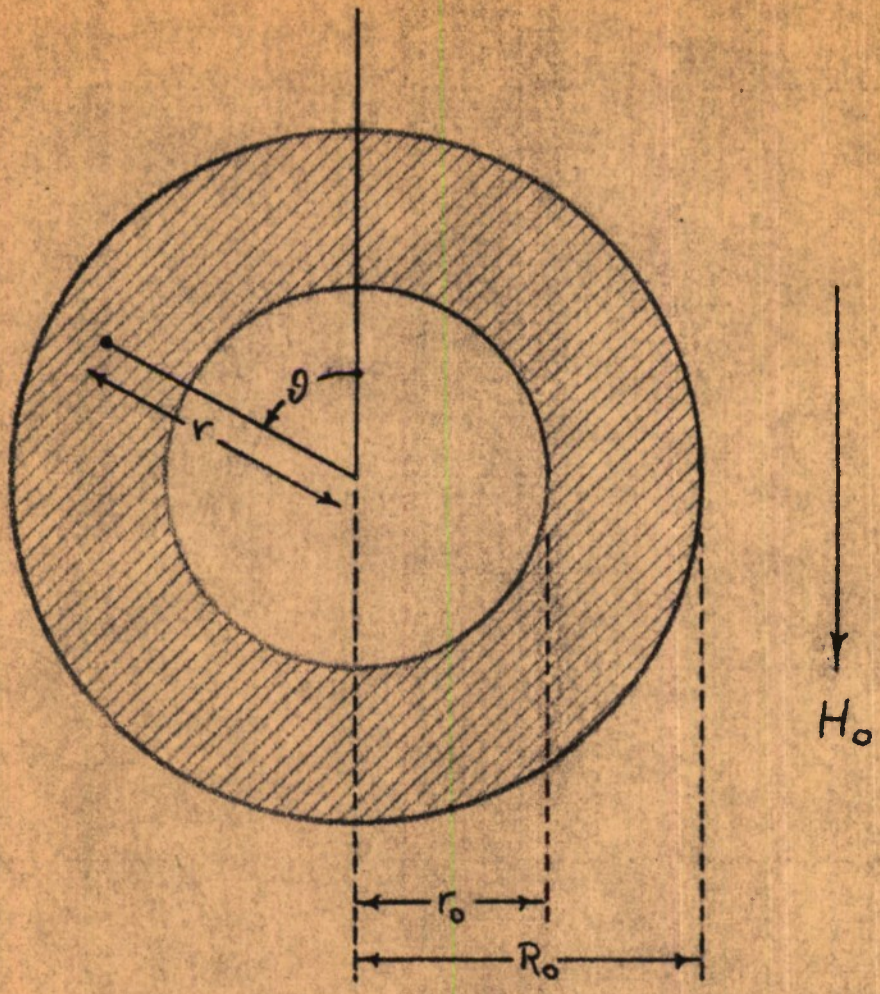

Figure 1. Definitions of geometrical parameters for the analysis of the d-c magnetization of a ferromagnetic tube.

tion may be expressed as follows: let

$$\frac{r}{R_o} = \rho \quad , \quad \frac{\mu-1}{\mu+1} = \nu \tag{16}$$

Then the potential V within the material of the tube is

$$V = H_o \frac{2R_o}{\mu+1} \left[\frac{\rho + \nu \rho_o^2/\rho}{1-\nu^2 \rho_o^2} \right] \cos\vartheta \quad , \quad \frac{r_o}{R_o} < \rho < 1 \tag{17}$$

The field $\underline{H}$ is

$$\begin{bmatrix} H_r \\ H_\vartheta \end{bmatrix} = H_o \frac{2}{(\mu+1)(1-\nu^2 \rho_o^2)} \begin{bmatrix} -(1-\nu\rho_o^2/\rho^2) & \cos\vartheta \\ (1+\nu\rho_o^2/\rho^2) & \sin\vartheta \end{bmatrix} \tag{18}$$

The magnitude $4\pi M$ of the magnetization is

$$4\pi M = H_o \frac{2\nu}{1-\nu^2\rho_o^2} \sqrt{1+\nu^2 \frac{\rho_o^4}{\rho^4} - 2\nu \frac{\rho_o^2}{\rho^2} \cos 2\vartheta} \tag{19}$$

As an illustration of the effect of the tube geometry, we evaluate $4\pi M$ in the extreme cases in which the tube becomes a rod ($\rho_o \to 0$) and in which the wall becomes very thin ($\rho_o \to 1$).

	ρ_o	$\vartheta = 0, \pi$	$\vartheta = \pi/2, 3\pi/2$
rod	0	$2\nu H_o$	$2\nu H_o$
thin-walled tube	1	$H_o \frac{2\nu}{1+\nu}$	$H_o \frac{2\nu}{1-\nu}$

For the low-field situation in which the material is only partially magnetized we may assume that μ is much greater than unity ($\mu >> 1$, $\nu \cong 1$). The table shows that the magnetization at the "top" and "bottom" ($\vartheta = 0, \pi$) of the thin-walled tube has nearly the same low value as that for the most unfavorable case of demagnetization, namely a thin sheet mag-

netized perpendicularly to its surface, while at the "sides" ($\vartheta = \pi/2,\ 3\pi/2$) it takes on large values, as for a thin sheet magnetized in its plane.

The maximum benefit of this effect occurs when the tube wall is quite thin: $\rho_o = r_o/R_o$ ought to be of the order of 0.9 or so. If the wall is thicker than this, the magnetization is still large at the outer surface ($\rho \cong 1$), but declines rapidly and at the inner surface ($\rho = \rho_o$) attains only a slightly enhanced value as compared with that for a rod. Thin-walled tubes are also advantageous from the point of view of broadbanding[8]; their disadvantages lie in the problems of producing a well-matched transition to conductive-wall guide and in maintaining good dielectric-waveguide propagation characteristics. Both of these problems are soluble. The only ineluctable disadvantage is that the outer diameter of the tube may be so large as to constitute somewhat of an inconvenience for some purposes: whereas for a solid rod the optimum diameter is of the order of a half-wavelength in the dielectric, for a tube the diameter must be increased as the wall is made thinner, approaching approximately a half-wavelength in air.

4D. Permeability variation in partially-magnetized ferrite.

As discussed in Sec. 3, among the objectives of the program was that of producing a variation in magnetization by utilizing the magnetostatic properties of a tube, analyzed in the above paragraph 4C, and to use this state of magnetiza-

tion as a means for obtaining anisotropic propagation by virtue of the low-field permeability variation. We were not able to observe this effect conclusively, although we believe that it can be made to take place once the more superficial obscuring effects such as interferences are ameliorated and a thorough search for the most suitable ferrite composition can be systematically carried out. The following discussion summarizes the nature of the phenomenon in question.

The permeability μ appearing in the Polder tensor for a gyromagnetic medium, equation (7), is given in terms of magnetization $4\pi M$, field H, and frequency ω by the expression (equation 8)

$$\mu = 1+\frac{4\pi\gamma^2 MH}{\gamma^2 H^2-\omega^2} \qquad (20)$$

When μ is measured at small values of H, it is found that in the case of polycrystalline materials having $4\pi M$ in the neighborhood of ω/γ the permeability is appreciably less than unity at H = 0 and rises rapidly to values near unity as the material is magnetized. The phenomenon is illustrated in Figure 2. There is also a dissipative effect, known as the low-field loss[12]. It is possible to interpret these within the scope of equation (20) provided the magnetic field H which appears there is correctly interpreted as the effective internal field, including the local fields generated by magnetic disorder in the polycrystalline material as well as the applied field. Even in the completely unmagnetized

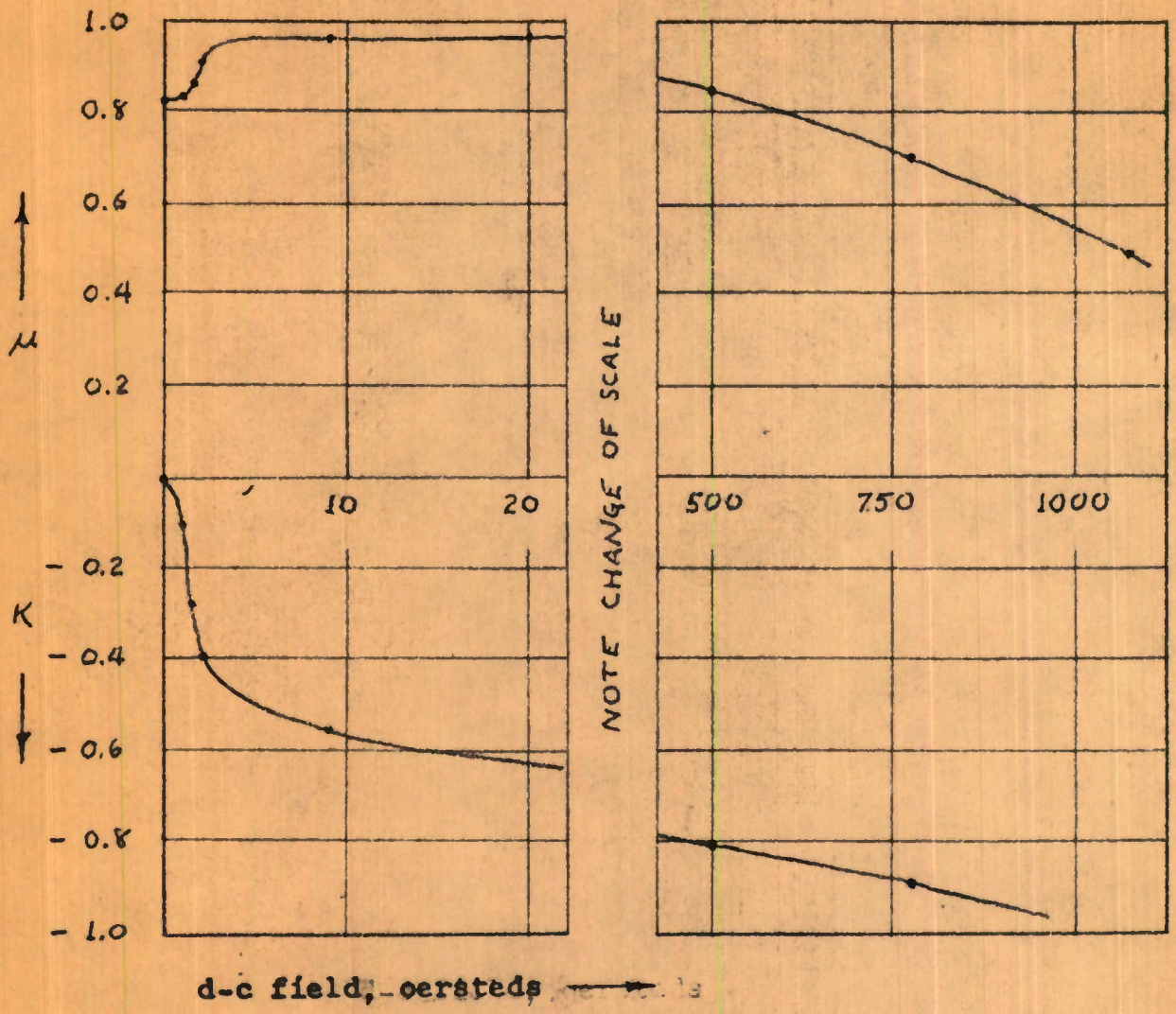

Figure 2. Experimental data showing the dependence of μ and κ on d-c field in the low and intermediate ranges. Data from reference 11; $4\pi M_s$=1700 gauss, frequency=6.2 KMc.

state, where both $4\pi M$ and H are null on the average, the average of their product is not zero in general because of the strong correlation between them. In materials of higher values of saturation magnetization both the reactive and the dissipative variations in μ become more pronounced. With skillful choice of material it is possible to obtain an appreciable reactive variation in μ while incurring only small losses.

The physical origin of the phenomenon is to be found in the microcrystalline structure of the sintered material. At H = 0 the crystallites are magnetized in random orientations; the boundaries between magnetic domains act as sources of magnetostatic (demagnetizing) fields which are effective in controlling the permeability. Indeed, if the saturation magnetization is in the neighborhood of

$$4\pi M = \frac{\omega}{\gamma} \tag{21}$$

the range of these demagnetizing fields may extend from zero up to magnitudes sufficient to place some parts of the material in the condition of ferromagnetic resonance. The expression (20) shows that μ ranges from zero to large values, both positive and negative, over this interval of H. To predict the mean value of μ with the aid of equation (20), it is necessary to average the quantities $4\pi MH$ and H^2 over the volume of the specimen; the net reactive effect, a decrease in the real part of μ, occurs primarily because of the strong geometrical correlation between the vector quanti-

ties $4\pi\underline{M}$ and $\underline{H}$.

When a field is applied to the specimen, magnetization becomes more orderly and the random internal demagnetizing fields gradually disappear. The permeability increases at first and ultimately takes up the dependence on H in agreement with Polder's expression and corresponding to the fixed value of saturation magnetization $4\pi M_s$. The entire process takes place in the range of field values from zero to less than 100 oersteds. This mechanism provides a means for obtaining a magnetically variable effective permeability and thereby, with proper attention to the microwave characteristics of the structure, a variable velocity of propagation, which leads to the desired phaser action.

5. Scattering analysis.

5A. Scattering by the ferrite section.

We consider first the effect of mismatches at the ends of the ferrite-loaded section on the phase and amplitude of transmission, assuming that the quarter-wave transducers at the input and output ends are perfect.

Radiation of unit amplitude entering the input transducer polarized in the x-direction (the E-plane of rectangular guide) is converted into a circularly-polarized wave whose components in the directions ϑ and $\vartheta+\pi/2$ of the principal axes p and s, respectively, of the half-wave section are given by the formulation of Sec. 4A as

$$\begin{bmatrix} A_p \\ A_s \end{bmatrix} = \frac{1}{\sqrt{2}} e^{-i\vartheta} \begin{bmatrix} 1 \\ -i \end{bmatrix} \tag{22}$$

Each component undergoes scattering by the half-wave section; since they are normal modes they do not interact within the section, provided (as we shall assume) there is no exchange of energy between them due to reflection from the ends. This assumption is valid if the symmetry of the matching structures at the ends conforms to that of the magnetized ferrite itself. The transmitted signals at the output of the half-wave sections are of amplitudes E_p and E_s:

$$E_p = A_p s_p s_p' \frac{e^{-i\beta_p l}}{1-r_p'^2 e^{-2i\beta_p l}} \tag{23}$$

and similarly for E_s with p replaced by s. The coefficients r, s, and s′ define the scattering at the ends, as indicated in Fig. 3. At the output the two transmitted signals are reconverted into the single rectangular guide mode of amplitude E,

$$E = \frac{1}{\sqrt{2}} e^{-i\vartheta}(E_p - iE_s) \qquad (24)$$

$$= \frac{1}{2} e^{-2i\vartheta}\left[\frac{s_p s_p' e^{-i\beta_p \ell}}{1-r_p'^2 e^{-2i\beta_p \ell}} - \frac{s_s s_s' e^{-i\beta_s \ell}}{1-r_s'^2 e^{-2i\beta_s \ell}}\right]$$

From this result it may be seen that the amplitude of transmission E is reduced if either or both modes encounter mismatches ($r_p, r_s \neq 0$) and that the frequency-dependence of phase may also be disturbed in more or less complicated ways, depending on the phases and amplitudes of the scattering coefficients. It is to be noted, however, that the dependence of phase on the orientation ϑ of the d-c field is not affected by these disturbances. In anticipation of the next subsection, in which we consider the effects of imperfections in the quarter-wave transducers, we observe that equations (23) and (24) specify three circumstances in which the half-wave section transforms a circularly-polarized input wave into an elliptically-polarized output: one, the propagation constants β_p and β_s do not give the proper half-wave phase differential $(\beta_p - \beta_s)\ell = 2\delta\ell = \pi$; two, the corresponding scattering coefficients for the p and s modes differ from one another in phase or amplitude; three, the dissipation (which may be represented in the usual way by adding an imaginary part to the propagation

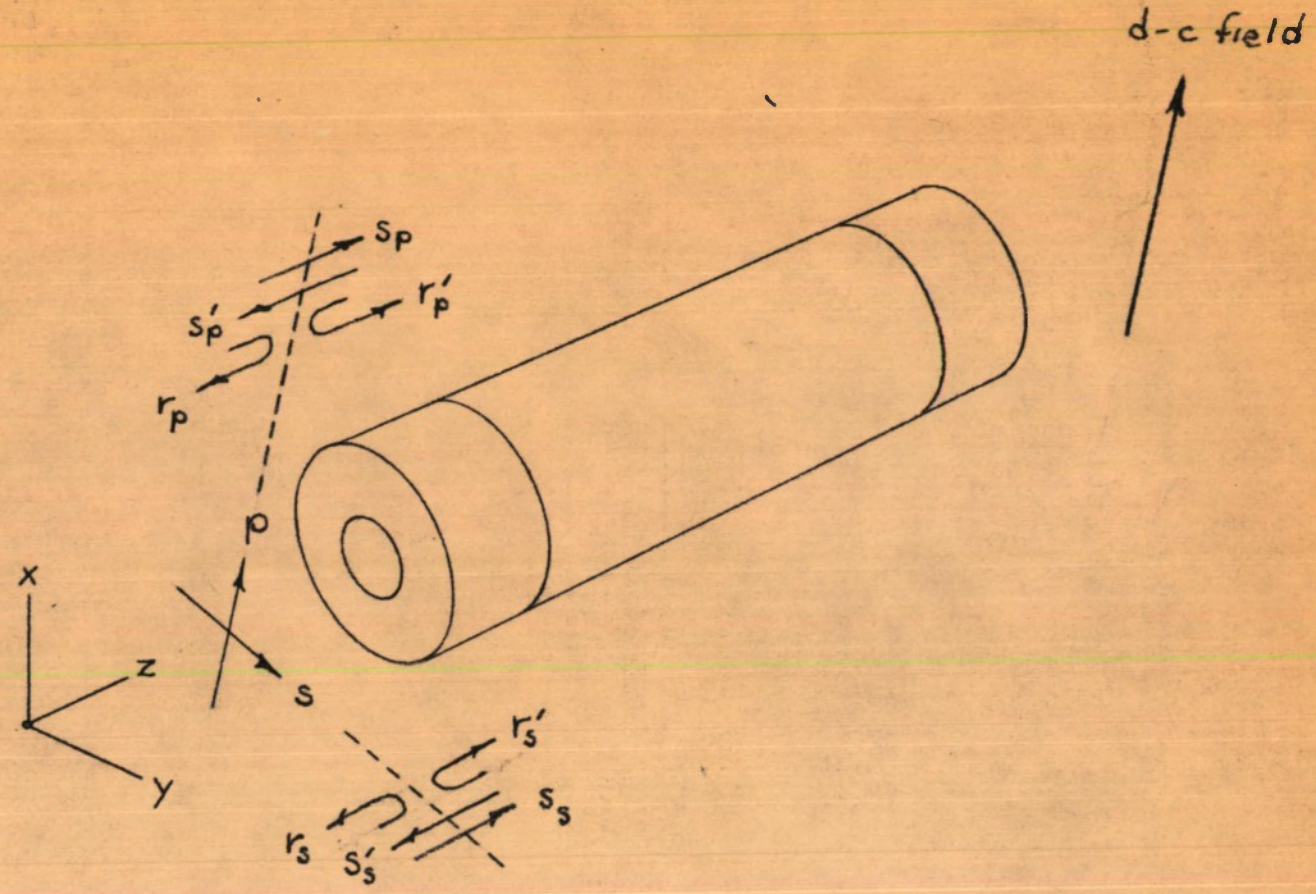

Fig.3. Diagram of the ferrite half-wave section, showing the definitions of the scattering coefficients r,r',s, and s' in the two modes, p and s, for the ends of the section.

constant) is different for the two modes.

5B. Scattering by the quarter-wave transducers.

As discussed in Sec. 6, the contributions from all of the disturbances enumerated above can not account for the form and magnitude of the observed deviations from ideal performance. We shall now show that these small effects show up in greatly magnified form if the input and output quarter-wave transducers are imperfect.

We consider a quarter-wave transducer connected to single-mode (rectangular) guide at its input end and to two-mode (circular) guide at its output end. If the transducer were perfect, then a signal of amplitude A_x arriving at the input end polarized in the x-direction would be converted to a circularly-polarized signal whose components A_p, A_s in the directions of the principal axes p,s of the two-mode guide would be

$$\begin{bmatrix} A_p \\ A_s \end{bmatrix} = \frac{1}{\sqrt{2}} e^{-i\vartheta} A_x \begin{bmatrix} 1 \\ -i \end{bmatrix} \tag{25}$$

where ϑ denotes the orientation of the principal axes with respect to the input axes x,y. It is convenient to use the circularly-polarized components A_+, A_- in the two-mode region, where

$$A_{\pm} = A_p \pm iA_s \tag{26}$$

then

$$\begin{bmatrix} A_+ \\ A_- \end{bmatrix} = \sqrt{2}\, e^{-i\vartheta} A_x \begin{bmatrix} 1 \\ 0 \end{bmatrix} \tag{27}$$

Signals of amplitudes B_+, B_- arriving from the other direction would be converted to linearly-polarized components

$$\begin{bmatrix} B_x \\ B_y \end{bmatrix} = \frac{1}{\sqrt{2}} \begin{bmatrix} e^{-i\vartheta} B_- \\ -ie^{i\vartheta} B_+ \end{bmatrix} \tag{28}$$

A loss film placed at the single-mode end of the transducer would absorb the component B_y which is polarized in the non-propagating orientation.

Various imperfections may be present in an actual embodiment of this device. It may not be exactly a quarter-wave long as measured by the phase differential between its normal modes; the normal coordinates may not be oriented at exactly 45° with respect to the polarization of the incoming signal. In the presence of these imperfections, the input signal A_x is converted to the components

$$\begin{bmatrix} A_+ \\ A_- \end{bmatrix} = \sqrt{2}\, A_x \begin{bmatrix} (1+iw)e^{-i\vartheta} \\ -(v-iw)e^{i\vartheta} \end{bmatrix} \tag{29}$$

where v and w denote respectively the errors in the differential phase $\delta\varphi$ and in the orientation ϑ_0; both are assumed to be small:

$$\delta\varphi = \frac{\pi}{2}+v \quad , \quad \vartheta_0 = \frac{\pi}{4}+w \tag{30}$$

Further, the loss film may not completely absorb the component B_y of a signal coming from the two-mode region. The component in question is

$$B_y = -i\frac{1}{\sqrt{2}}\left[(1-iw)e^{i\vartheta}B_+ + (v+iw)e^{-i\vartheta}B_-\right] \tag{31}$$

Let t denote the reflection coefficient for reflection of this cross-polarized signal back into the transducer. Then, considering both the signal A_x originally incident on the input end and the signal generated by the reflection tB_y of waves returning from the output end, the sum is

$$\begin{bmatrix} A_+ \\ A_- \end{bmatrix} = \sqrt{2}A_x \begin{bmatrix} (1+iw)e^{-i\vartheta} \\ -(v-iw)e^{i\vartheta} \end{bmatrix} - t\left[(1-iw)e^{i\vartheta}B_+ + (v+iw)e^{-i\vartheta}B_-\right] \begin{bmatrix} (v+iw)e^{-i\vartheta} \\ (1-iw)e^{i\vartheta} \end{bmatrix} \tag{32}$$

We may now apply the result (32) to the complete phaser assembly, composed of the ferrite half-wave section, whose principal axes are oriented at ϑ, with quarter-wave transducers at each end. To illustrate the nature of the effect of the various imperfections on the overall phase and amplitude of the transmitted signal, it is not necessary to treat the scattering by the ferrite section with complete generality. We shall bear in mind that reflections in that part of the structure would add still further complications, and shall include for present purposes only the property, represented by equation (24), of distrubing the phase and amplitude of transmission. The net effect is that an incident signal which is circularly-polarized in one sense is

converted into an output which is predominantly in the opposite sense but contains a component in the original ("wrong") sense. This "wrong" wave is then subject to the reflection t, treated above, when it passes through the quarter-wave transducer. From equation (24) it can be seen that the disturbance is frequency-dependent in that it depends on the average electrical length $\beta\ell$ of the ferrite section.

If the ferrite section were perfect, it would convert the incident circularly-polarized waves A_+ and A_- of equation (32) into transmitted waves E_+ and E_- according to

$$\begin{bmatrix} E_+ \\ E_- \end{bmatrix} = e^{-i\beta\ell} \begin{bmatrix} \cos\delta\ell & -i\sin\delta\ell \\ -i\sin\delta\ell & \cos\delta\ell \end{bmatrix} \begin{bmatrix} A_+ \\ A_- \end{bmatrix} \qquad (33)$$

where $2\delta\ell$ is the differential electrical length, as expressed in equation (4), et. seq., Sec. 4A. Ideally, $\delta\ell = \pi/2$, so that the matrix of (33) reduces to a simple permutation of + and - circularly-polarized waves. We shall replace that matrix by

$$\begin{bmatrix} E_+ \\ E_- \end{bmatrix} = e^{-i\beta\ell} \begin{bmatrix} a & -ib \\ -ib & a \end{bmatrix} \begin{bmatrix} A_+ \\ A_- \end{bmatrix} \qquad (34)$$

where a and b are left unspecified except that they must, of course, satisfy the requirement of energy conservation. In the ideal case they would agree with (33), but in general

they will be assumed to contain the phase and amplitude disturbances described by equation (24).

Corresponding to equation (32) we have a similar expression relating the signals F_+ and F_- reflected at the output transducer to the signals E_+ and E_- incident upon it. The transfer matrix of equation (34) connects the F's to the B's in the same way it connects the A's to the E's. Thus, we have a system of equations describing the superposition of waves resulting from the group of imperfections contemplated, and leading to an overall transmission E_x in the rectangular guide at the output end.

We shall carry through the calculation in the simplest case, namely that the quarter-wave transducers are perfect in the sense that the errors v and w of equation (30) are zero, but retaining the reflection, specified by the coefficient t, of cross-polarized waves as discussed above (equation 31 et seq.). We have from (32),

$$\begin{bmatrix} A_+ \\ A_- \end{bmatrix} = \sqrt{2}A_x e^{-i\vartheta} \begin{bmatrix} 1 \\ 0 \end{bmatrix} - tB_+ e^{2i\vartheta} \begin{bmatrix} 0 \\ 1 \end{bmatrix} \tag{35}$$

As in (34), $B_+ = e^{-i\beta l}(aF_+ - ibF_-)$ (36)

Thus, $$\begin{bmatrix} A_+ \\ A_- \end{bmatrix} = \sqrt{2}A_x e^{-i\vartheta} \begin{bmatrix} 1 \\ 0 \end{bmatrix} - te^{i(2\vartheta-\beta l)}(aF_+ - ibF_-) \begin{bmatrix} 0 \\ 1 \end{bmatrix}$$

Similarly, for the waves F_+ and F_- reflected from the

output transducer,

$$\begin{bmatrix} F_+ \\ F_- \end{bmatrix} = -te^{i(2\vartheta-\beta\ell)}(aA_+ - ibA_-)\begin{bmatrix} 0 \\ 1 \end{bmatrix} \tag{38}$$

Equations (37) and (38) are to be solved simultaneously for A_+ and A_-; from this solution the transmitted wave amplitude E_x can be constructed:

$$E_x = \frac{1}{\sqrt{2}} e^{-i\vartheta}(-ibA_+ + aA-) \tag{39}$$

The solution is

$$E_x = -iA_x e^{-i(2\vartheta+\beta\ell)} b\left[\frac{1+(a^2+b^2)t^2e^{2i(2\vartheta-\beta\ell)}}{1+b^2t^2e^{2i(2\vartheta-\beta\ell)}}\right] \tag{40}$$

which we may write in the form

$$E_x = -iA_x e^{-i(2\vartheta+\beta\ell)}\left[\frac{b}{1 - \dfrac{a^2t^2e^{2i(2\vartheta-\beta\ell)}}{1+(a^2+b^2)t^2e^{2i(2\vartheta-\beta\ell)}}}\right] \tag{41}$$

Our object in exhibiting E_x in this form is to show its resemblance to the situation contemplated in the analysis of interference effects in Faraday rotation (reference 13). Here, as there, we are led to an expression for transmission in which there appears a fraction in the denominator, ordinarily small, but taking on relatively large values at frequencies for which the magnitude of its own denominator passes through a minimum. As shown in the reference cited, the shape (frequency-dependence) of these "dips" has a character agreeing closely with those we have observed. In the pre-

sent case, if the ferrite section were perfect we should have a = 0, and the effect would be absent; or, if the cross-polarized waves at the ends of the transducers were perfectly terminated, we should have t = 0 and again the interference effect described by (41) would be absent, although the smaller disturbances in phase and amplitude described by equation (24) would still be present. The two disturbances together yield strong amplitude and phase fluctuations whose characteristics, discussed in Sec. 6, agree qualitatively with the prediction (41). If we allow for the additional imperfections discussed above, such as the deviation from quarter wavelength and from 45° orientation, with the further complication that the errors in one quarter-wave transducer may be expected to differ from those in the other, comparison of the above scattering analysis with the observed behavior suggest that all the undesirable features of insertion loss, phase, and match over the frequency range studied could be accounted for.

A full appreciation of the intricate nature of the interaction between the ferrite half-wave section and the quarter-wave transducers came to us in the latter stages of the program; in fact, it was only after a considerable amount of progress had been made on matching of the ferrite to the conductive guide that the persistent features became clear enough to be analyzed. Although improvements in the transducer structure were carried out, it is clear from comparison of our latest data with the above analytical results

that further refinements are called for, and that they will yield materially improved phaser performance.

In early stages of the investigation measurements were performed using linearly polarized signals; simple quarter-wave plates were added later. As the need for more precise control of the polarization developed, step-transformer quarter-wave plates of an improved design due to R.D. Tompkins[14] and P.J. Allen were constructed and used in the subsequent work. The plates and their relation to the assembly are shown in the photographs, Fig. 4. Tests on the quarter-wave plates themselves showed that they are well adapted for work in the lower half of X-band. Their performance under one such test, measurement of the output amplitudes in two mutually orthogonal polarizations, is shown in the recorder tracing, Fig. 5. The amplitudes are equal, and near the ideal value of 3 db, at about 9.6 KMc. They slope gradually from this value in the expected way at higher and lower frequencies. For a full characterization of the transducer performance, the phase relation between the two components was studied and adjusted to produce circular polarization.

A number of attempts were made to build satisfactory loss films (see Fig. 4B). The structure and placement of the films most recently used appeared to be reasonably good for laboratory work. Having seen more clearly the nature and importance of defects in this element, we would devote special attention to matching and other details in the design before proceeding with further work on the phaser.

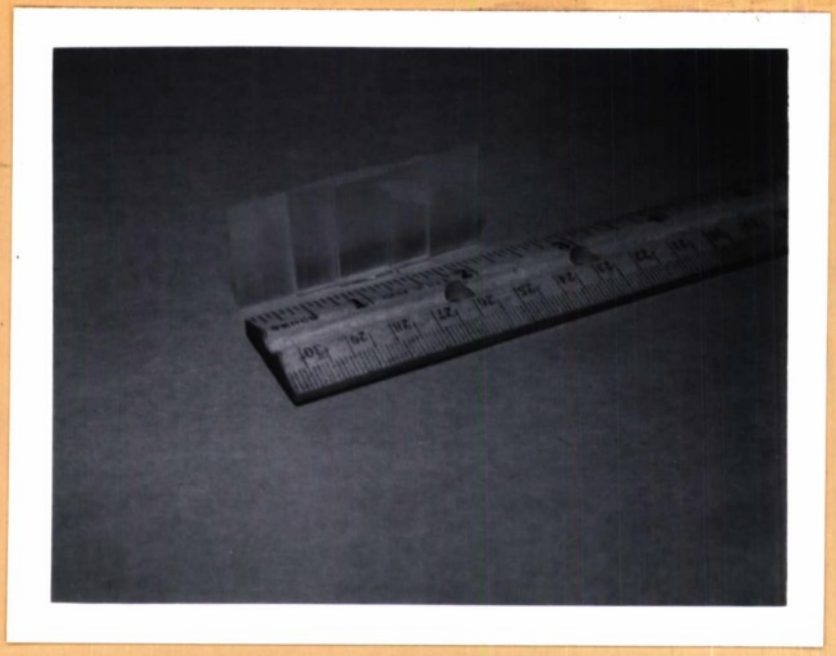

4A. The dielectric step-transformer quarter-wave plate.

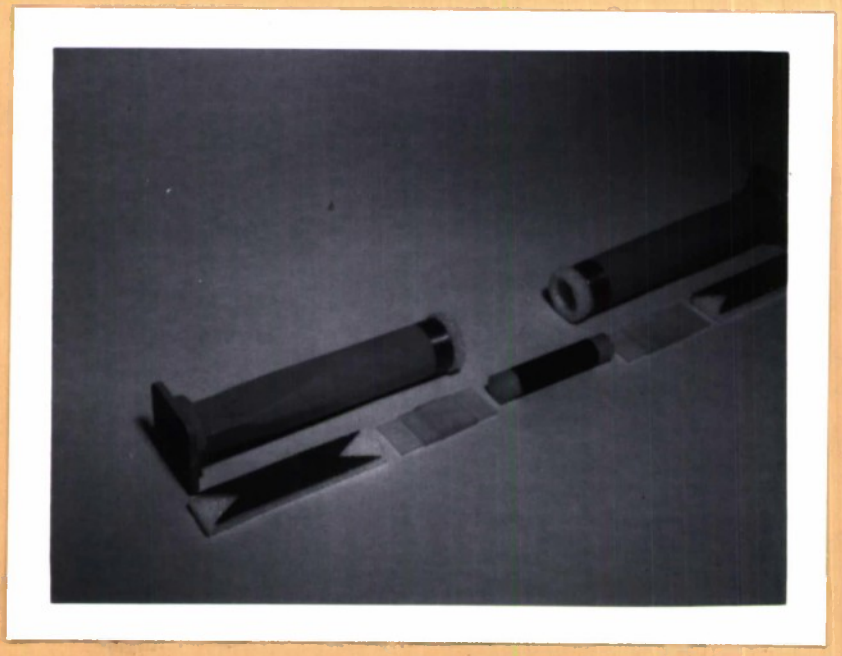

4B. Exploded view of ferrite with matching elements, dielectric quarter-wave plates, and terminations.

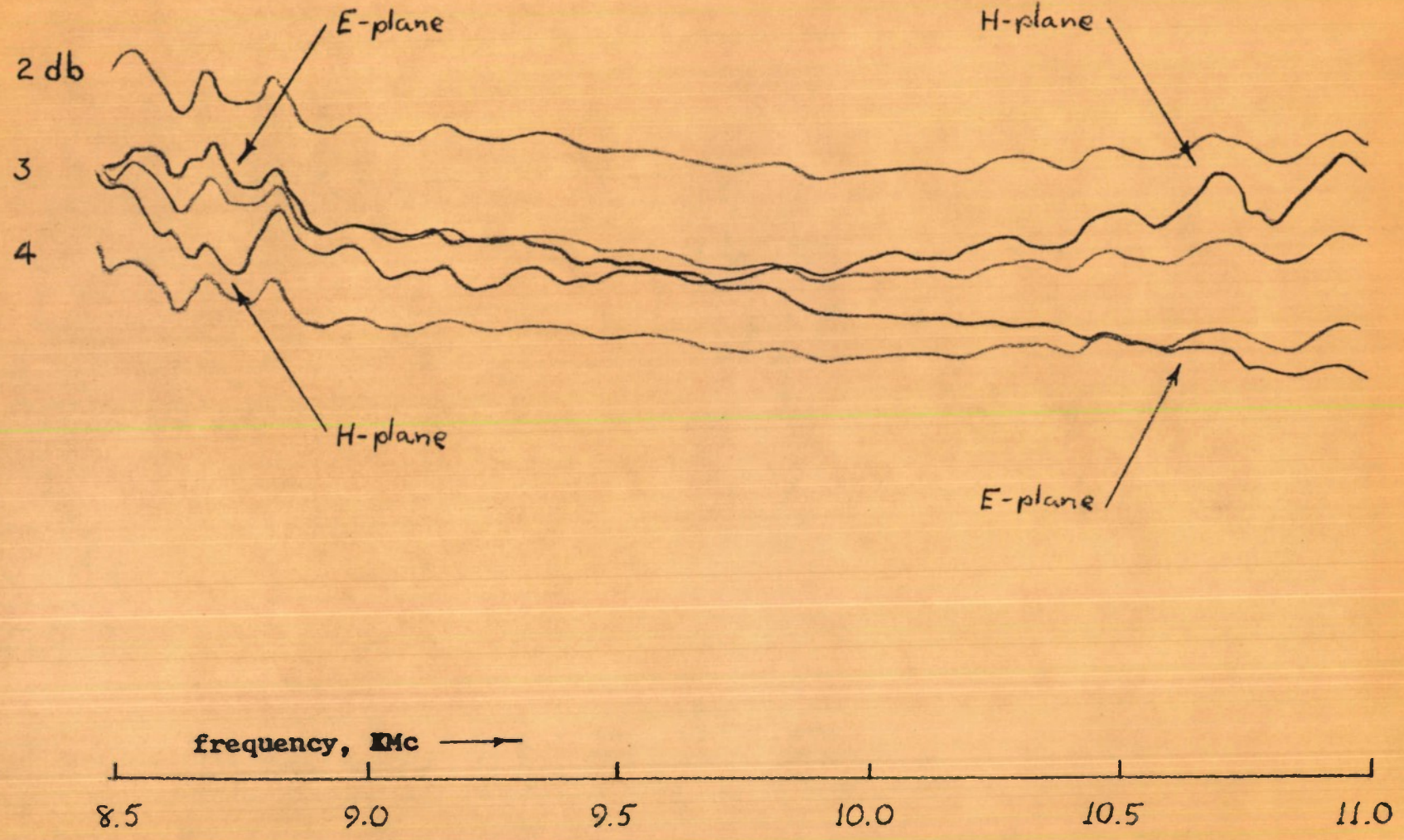

Figure 5. Performance of a quarter-wave transducer, measured by observing the amplitudes of waves polarized in the E- and H-planes at the output; the input signal is E-polarized.

6. Experimental results.

6A. Phase, insertion loss, and match.

Performance of the rotating-field phaser showing the characteristics inherent in this device has been observed. The results for a particular experimental assembly are shown in Fig. 6. The graph gives the insertion loss, phase, and VSWR as functions of orientation ψ of the magnetic field, measured at 9.36 KMc. Details of the ferrite half-wave plate structure and quarter-wave transducers are shown in Figs. 4 and 10.

The data of Fig. 6 show, at the top, insertion loss averaging about 1 db, with a periodic variation having a total excursion of about 0.5 db as ψ is varied. This loss includes that of the quarter-wave transducers which is difficult to evaluate separately; further discussion of this part of the problem will appear below. The phase of the transmitted signal, indicated by the two sloping solid lines, obeys the linear law of variation (equation 6) to a fair approximation, although it contains an S-shaped deviation which at its worst (around $\psi = 120^\circ$) departs by about 25° from the theoretical value. Part of this error is not intrinsic to the device but is characteristic of the measurement method (see Sec. 7) and is associated with the VSWR, shown by the dashed curve. The mismatch varies periodically with ψ between a maximum of 1.58/1 and a minimum of 1.35/1. That part of the deviation which is intrinsic results from a combination of small but significant imperfections; genera-

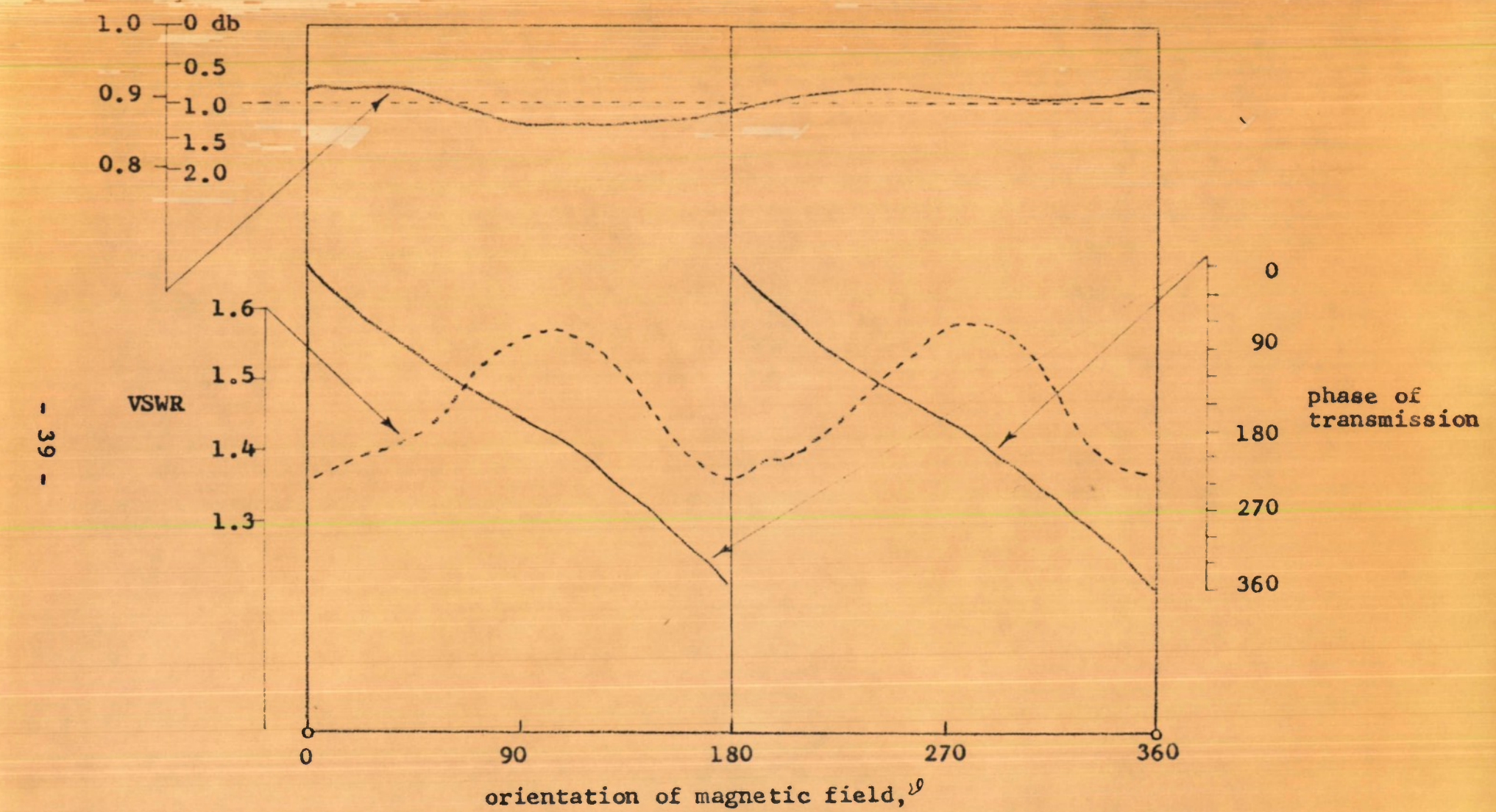

Fig. 6. Insertion loss, phase, and VSWR of the rotating-field phaser vs. angle of orientation ϑ of magnetic field; frequency, 9.36 KMc.

tion of a slightly elliptic, rather than circular, polarization by the transducers, incomplete absorption of the cross-polarized component appearing at the rectangular input and output guides, imperfect matching at the ends of the ferrite section, and a small difference in the damping of the two normal modes of the ferrite.

The selection of the frequency 9.36 KMc at which the data of Fig. 6 were taken was dictated by the frequency-dependence of insertion loss, shown in Fig. 7. The magnet was oriented at 0^{o} for that measurement, and the magnitude of the d-c field was adjusted to minimize insertion loss. The figure shows that the transmission undergoes a considerable amount of variation; the regular structure of this frequency-dependence is not apparent in Fig. 7 but emerges more clearly in other examples, shown in the recorder tracings, Figs. 8 and 9. The insertion loss values appearing in these figures include losses in all parts of the assembly, including the experimental-absorbing cards at the ends of the quarter-wave tranducers on which further comment is presented below. The essential point illustrated by these figures is the fact that the insertion loss exhibits certain regular features. An envelope of relatively low loss (the dashed curve in Fig. 9) extends across a considerable band, reaching a minimum around 9.4 KMc where the quarter-wave plates exhibit their optimum performance. This envelope is broken at regular frequency intervals by persistent and well-defined dips in transmission. A considerable part of the research effort to date has been devoted to identifying

Fig. 7. Insertion loss vs. frequency of the rotating-field phaser assembly; magnetic field oriented at $\vartheta = 0^{o}$.

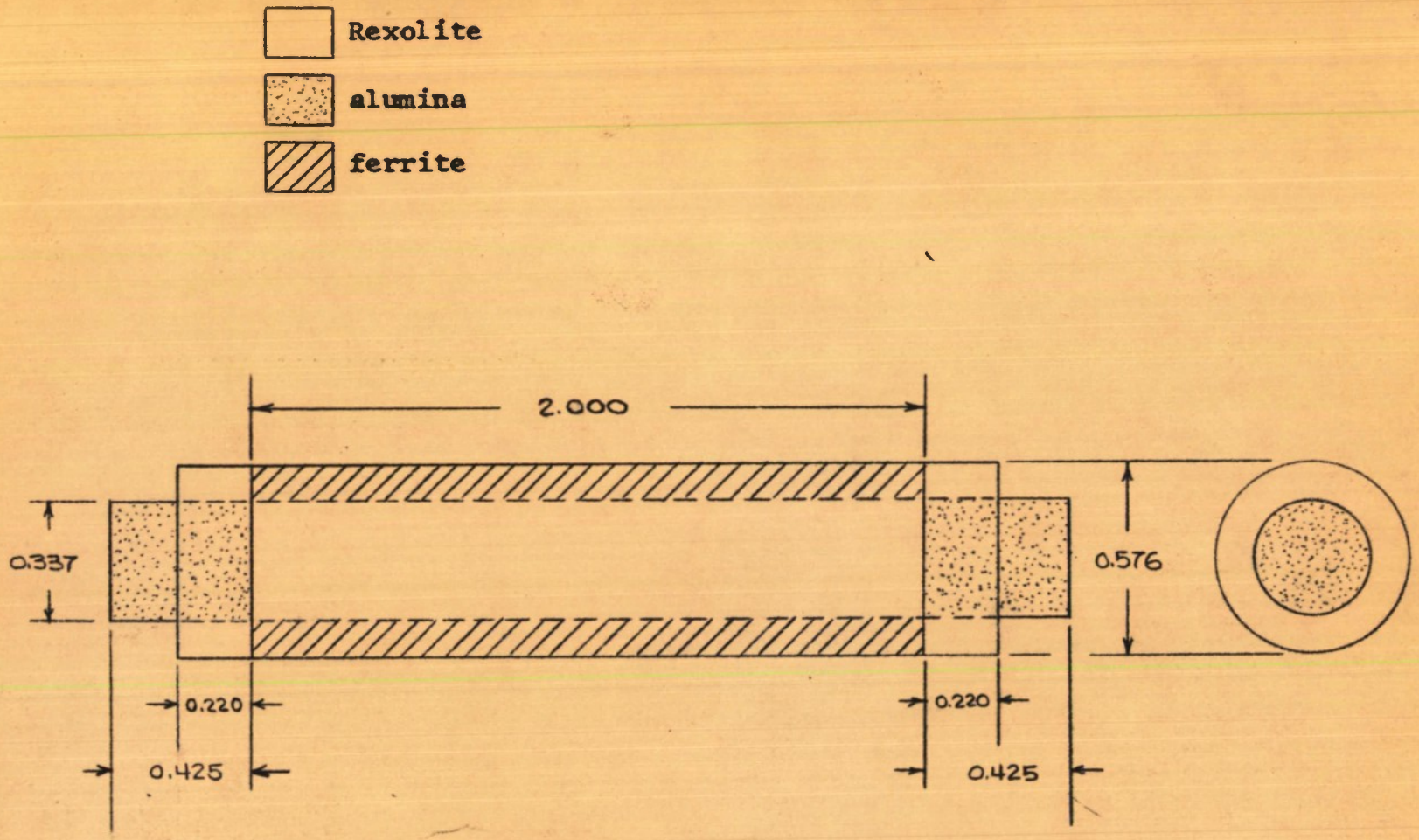

Fig. 7B. Configuration of ferrite tube and matching structures for data of Figs. 6 and 7.

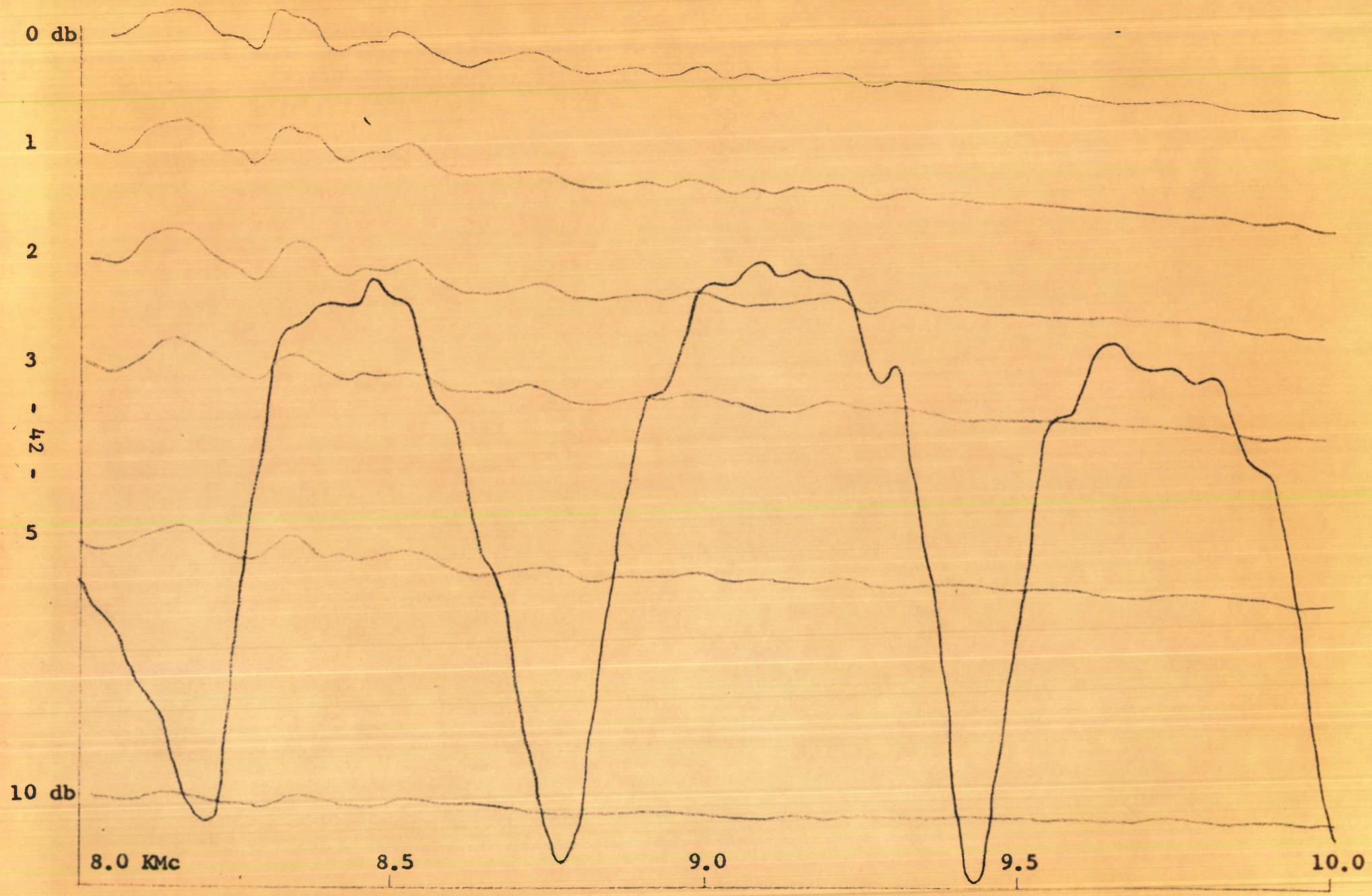

Fig. 8. Insertion loss vs. frequency of a rotating-field phaser assembly; example illustrating the regular repetition of interference peaks and dips.

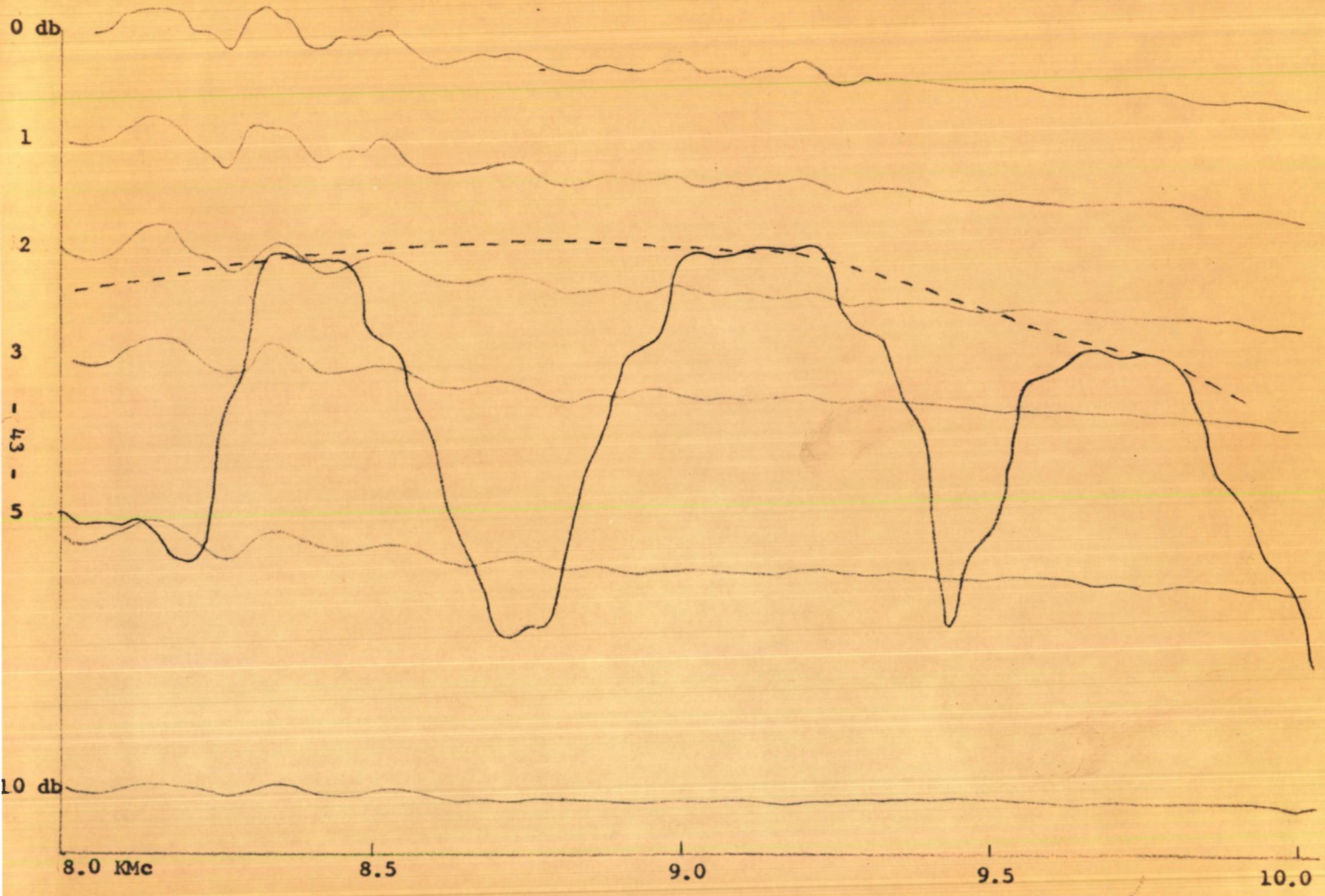

Fig. 9. Insertion loss vs. frequency of a rotating-field phaser assembly; second example with slightly improved matching of ferrite section.

these dips, which appear to be the only obstacle to the achievement of broadband phaser performance, and to modifying the design in an attempt to eliminate them. Comparison of Figs. 8 and 9 shows that the peaks are appreciably less deep in Fig. 9, reaching only about 6 db at most. The difference between the two cases is in the details of the matching structures at the ends of the ferrite tube: relocating of the alumina rods (see Fig. 10) a small distance from the tube produced the improvement. The insertion loss dips are sensitive to the orientation of the magnetic field, as illustrated in the recorder tracings of Fig. 11. An interpretation of this phenomenon is included in the discussion of scattering, Sec. 5.

Enough is known of the contributing effects to suggest strongly that this behavior is not intrinsic to the phaser principle being employed here but can be corrected. Experimental evidence to date has established that the insertion loss fluctuations are reactive (interference) effects resulting from a combination of imperfect matching at the ends of the ferrite section together with imperfections in the quarter-wave transducers; particularly the imperfect termination of signals in the "wrong" sense of circular polarization. Various experiments, including measurements of the radial extension of r-f fields around the ferrite, have demonstrated that they are not due to the excitation of spurious higher modes of propagation; nor are they associated with slight deviations from mechanical alignment of the parts

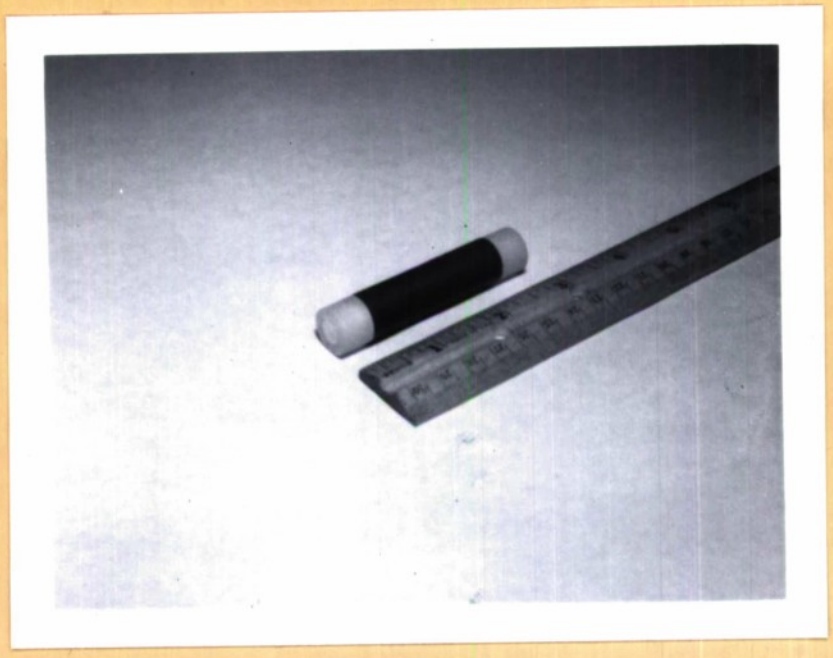

10A. Close-up view of the ferrite tube, with dielectric matching elements.

10B. Ferrite dielectric-waveguide half-wave section with adjoining quarter-wave transducers to rectangular X-band guide. The laboratory rotating magnet has been removed.

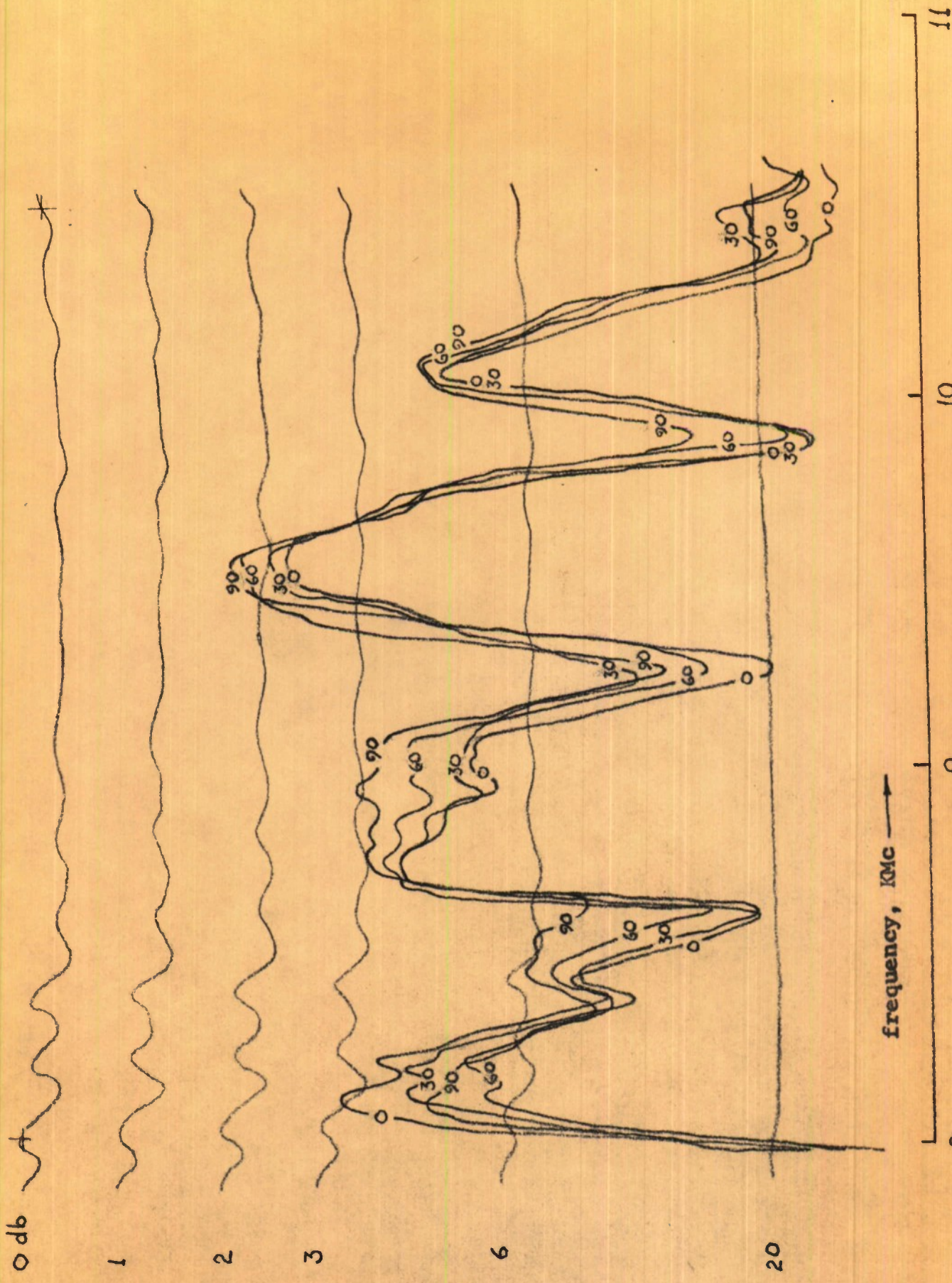

Figure 11. Recorder tracing illustrating the dependence of insertion loss on orientation of the d-c magnetic field.

of the assembly.

To account for the presence of these interferences and for their behavior under various experimental conditions, we observe, first, that the active ferrite half-wave element constitutes a two-mode transmission line and is therefore required to present a good match to incident waves in two different polarizations. A straightforward analysis of the scattering of the normal modes of propagation yields an expression for the amplitude and phase of the transmitted signal which shows that the departure from circular polarization of the transmitted wave at the output end of the half-wave section is under the control of the differential phase of the section and of the reflection coefficients for the two normal modes at the ends of the structure.

The polarization at the output end is perfectly circular provided the differential phase $(\beta_p - \beta_s)$ is precisely π and provided the scattering coefficients for the two modes are equal in phase and amplitude. The result of the analysis is given in Sec. 5 (equation 24).

Small deviations from this ideal combination of conditions would lead only to slightly increased insertion loss <u>if</u> the two quarter-wave transducers were themselves perfect. They may depart slightly from the requirement of $\pi/2$ differential electrical length without appreciable consequences; if, however, they do not present a quite well-matched termination to that component in the "wrong" sense of circular polarization generated by the accumulation

of small errors enumerated above, the multiple reflection of this spurious component is capable of producing very sharp fluctuations in transmission. This state of affairs is quite generally encountered in transmission-line circuits which are of the nature of a phase bridge, where the incident signal is split into two parallel channels and then recombined. That "trapping" of energy within the bridge circuit can give rise to sharp spikes of reflection has been demonstrated by us previously[13]. In the more familiar case of Faraday rotation the frequency-dependence of insertion loss conforms with excellent accuracy to the form predicted by equation (41), Sec. 5, for the transmission amplitude E. In the present case of the rotating-field half-wave section many of the same characteristics are present, at least qualitatively. The shape and regular repetitive character of the insertion loss dips, and their sensitivity to variations in magnitude and direction of the d-c field, as well as their response to changes in the matching and loss card structures, all support a picture of their origin as described above.

6B. Hysteresis.

Our investigation of hysteresis effects related to the question whether hysteresis in the d-c magnetization of the ferrite would cause uncertainty in the correlation between magnetic field orientation and phase of transmission.

The result of the measurements is that no such effect occurs; more exactly, that the phase obtained for a given setting of the magnet is unique to within the precision of the phase measurement, irrespective of the course of magnet rotation leading to the setting in question. The performance is illustrated in Fig. 12. The upper curve in the figure shows the phase as measured by observing the position of a standing-wave minimum in front of the device when a short-circuit plate is placed at the output (see Sec. 7 and Fig. 13A). With this curve as a reference, the deviation in position of the minimum was measured as the magnet was carried through several cycles over the range from $\vartheta = 90^{\circ}$ to $\vartheta = 180^{\circ}$. The lower curves show the deviations; they are within 0.4 mm which is of the same order as the uncertainty in minimum position. The deviations are also given in degrees; they are well under 2°. During the course of the measurement, the electromagnet current drifted slightly; the effect of this was also within the limit of measurement precision.

6C. Temperature effects.

Measurements of temperature effects were undertaken at a point in the program at which we felt that the insertion loss and phase fluctuations were under sufficient control to permit such a measurement. Our experience in these tests indicated that the temperature sensitivity tends to be satisfactorily small; we found, however, that it was not possible to obtain a truly reliable measure of temperature-

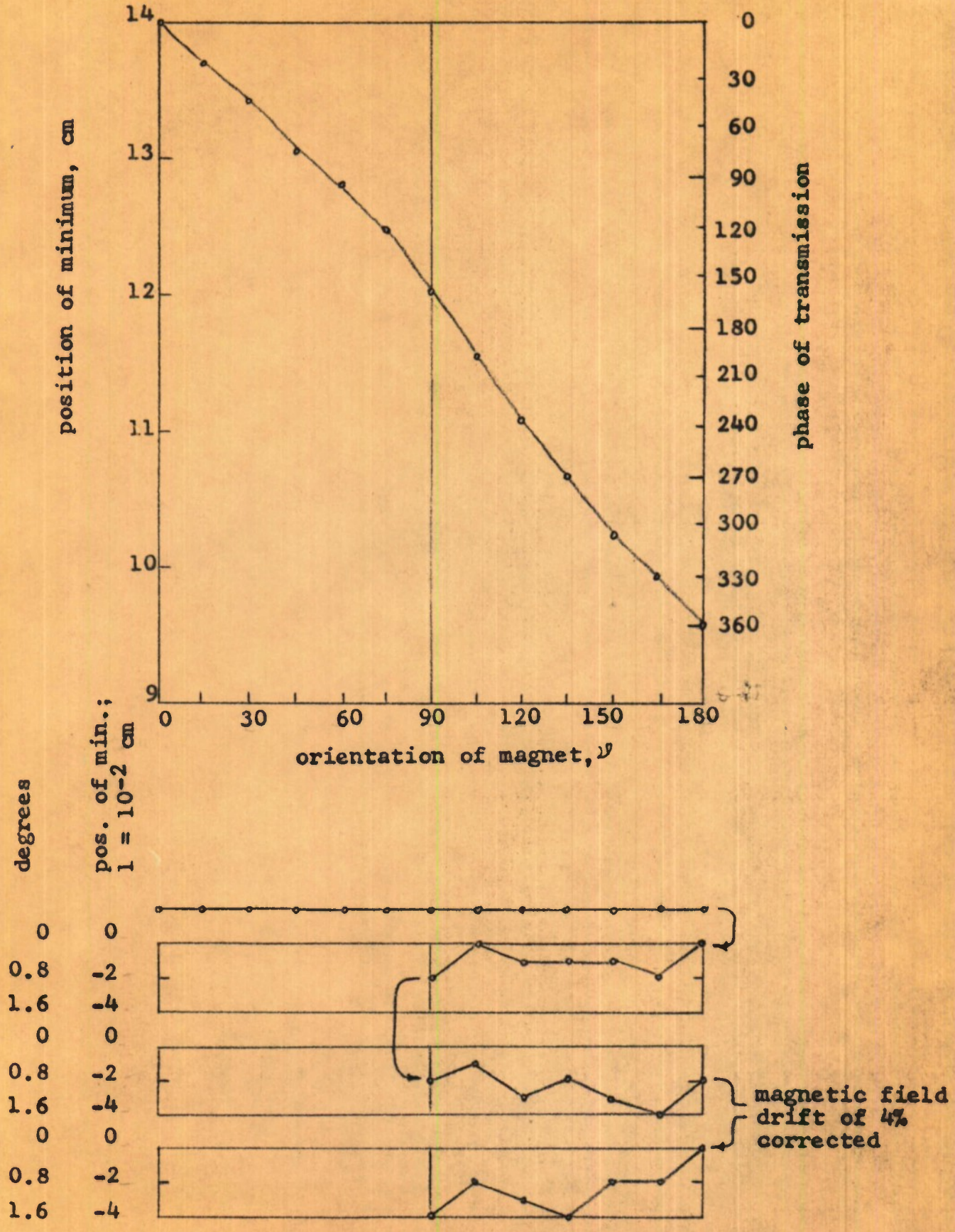

Fig.12. Phase of transmission. Lower curve shows deviation of phase in successive traversals of the $\vartheta = 90^\circ$ to $\vartheta = 180^\circ$ range.

dependence over a wide range because of the disturbing mismatch effects discussed earlier. Starting at 150°F, the overall phase (the quantity βL in equation 6, Sec. 4A) and the relative phase shift versus $\mathcal{V}$ were observed at a sequence of decreasing temperatures. The shift in βL was of the order of 0.1° per degree Fahrenheit at first, but the rate of change increased as the temperature declined, while the disturbances in insertion loss and phase-vs.-$\mathcal{V}$ increased. The behavior was such as to indicate that the frequency for optimum performance had shifted away from the test frequency (9.37 KMc). Examination at neighboring frequencies confirmed this. We conclude that there is room for optimism regarding the temperature sensitivity, but that it will be possible to perform a much more meaningful measurement after further improvement has been made in the obscuring reactive effects.

6D. D-c control field requirements.

The magnetic control field requirements have been in the range from 200 to 600 oersteds, with most of the significant data taken at fields of about 500 oersteds. These magnitudes suggest that the differential phase shift has been due almost entirely to gyromagnetic interaction rather than low-field effects. While such fields could be employed in practical devices if necessary, there still remains the possibility of reducing them considerably by further effort toward obtaining the optimum ferrite tube

geometry and the optimum ferrite composition.

The tube wall thickness should be reduced to bring the ratio ρ_o of inner to outer diameter (see Sec. 4C) to the range 0.8-0.9. This means that the outer diameter must be increased in order to sustain dielectric-waveguide propagation, and that the matching structure at the ends of the ferrite must be further refined. Because these changes might result in a ferrite diameter which is inconveniently large, some experiments were performed on composite structures containing additional dielectric (e.g., a ferrite tube filled with alumina or polystyrene). The results were inconclusive, again because of severe mismatch effects.

With regard to ferrite compositions suitable for study of low-field permeability variation effects at X-band, we find that the choice of materials is inconveniently narrow. The approximate rule specifying an upper limit to the saturation magnetization value at which the effect can be used is $4\pi M_s = \omega/\gamma'$, where γ' is the gyromagnetic ratio, $\gamma'/2\pi = 2.8$ Mc per oersted. For X-band, we obtain $4\pi M_s \sim 3560$ gauss. For lower values of $4\pi M_s$ the effect is less strong, but magnetic dissipative effects are also; thus the optimum value can be expected to lie somewhere in the range 2000-3000 gauss. In studying this problem, we found that nickel ferrites having suitable $4\pi M_s$ values were objectionably lossy at low fields, suggesting that the low-field loss effects[12] are more severe in these materials. Such behavior is not entirely unexpected; it correlates qualitatively with the known ferromagnetic resonance properties of nickel ferrites.

The amount of loss was, however, unexpectedly large. The magnesium-manganese ferrites, which are known[10,11] to exhibit the low-field reactive effects quite satisfactorily at somewhat lower frequencies (see Fig. 2), are limited in saturation magnetization to values below 2400 gauss. Most of our later work was done with a material of this type, but unfortunately our measurements showed that the effect we sought was not large enough to produce the desired low-field operation. It is reasonable to expect that further study of the available ferrites would identify one which combines characteristics close to those required for this application.

6E. Application of the phaser principle at L-band.

Our study directed toward finding ferromagnetic materials suitable for use in a rotating-field phaser for L-band involved the following problems:

a. to select ferrites and ferromagnetic garnets of appropriate compositions from among the materials now commercially available or expected to be so in the near future;

b. to investigate these materials experimentally at L-band with particular attention to their reactive and dissipative properties at low and intermediate values of d-c field;

c. to obtain estimates of the cost and to explore the problems associated with fabricating suitable specimens, such as tubes.

Four materials emerged as the most likely to be useful for the purpose; their significant characteristics

are summarized in Table I.

As shown in the Table, all of the materials showed a very conspicuous reactive permeability variation at low fields, but the three ferrites exhibited objectionally high values of magnetic loss. The magnetic loss tangent $\tan \delta_m = \mu''/\mu'$ for the best of the three, TT2-113, was about 1.0 at zero field and declined only to 0.25 before increasing again due to the onset of ferromagnetic resonance effects. The garnet MCL-300 was considerably better, $\tan \delta_m < 0.095$. Hence, irrespective of the other characteristics of the various materials, only the garnet could be considered a reasonably likely candidate for successful operation in a phaser.

Scaling from our experience at X-band, we estimated that a tubular specimen of the following dimensions would represent a good approximation to the final design: length, 8 inches; outer diameter, 4 inches; inner diameter, 2 inches or somewhat greater. Presses and furnaces large enough to make such a unit in one piece do not exist; we are confident, however, that a unit assembled from a number of smaller pieces machined to within reasonable tolerances would serve equally well. We obtained cost estimates in the following ranges: up to ten units, \$2100-\$2500 per unit; one hundred units, about \$2000 per unit. Some saving, perhaps 5 to 10%, might be effected if in production the parts could be molded to such close tolerances as to require no subsequent grinding. As a comparison of the relative

name	source	type	$4\pi M_s$, gauss	resonance line-width ΔH, oersteds	Curie temp., °C	g-value	dielectric constant ϵ	dielectric loss tangent $\tan \delta_\epsilon$	permeability at zero field μ'	permeability at zero field μ''	permeability at H=200 oe μ'	permeability at H=200 oe μ''
TT 1-103	T[a]	MgAl[b]	500	80	120	2	11.2	5×10^{-4}	~0	~1.06		
TT 2-113	T	NiAl	440	155	160	1.54	9	10^{-3}	0.45	0.47	1.1	0.25
TT 414	T	MgAl	600	90	100	2	11.5	5×10^{-4}	~0	~1.06		
MCL-300	M	YGa	300	55	125	2	11.7	1.6×10^{-3}	0.74	<0.07		

Notes a. sources: T=Trans-Tech, Inc., P.O. Box 457, Gaithersburg, Md.
M=Microwave Chemicals Laboratory, Inc., 282 Seventh Ave., New York, N.Y.

b. type: MgAl = magnesium-manganese-aluminum ferrite
NiAl = nickel-aluminum ferrite
YGa = yttrium-gallium-iron garnet

Table I. Characteristics of ferromagnetic materials relating to their use in an L-band rotating-field phaser.

costs of garnet and ferrite, a similar specimen made of ferrite would cost about 40% of the amounts quoted above.

Other questions relating to the development of an L-band unit were considered. They include: design of transducers for the generation of circular polarization, either of the quarter-wave type discussed in Sec. 5B or based on the properties of hybrid junctions or dual-mode transducers[14] ("through-plexers"); design of a compact, high-speed magnet structure to provide the control field; use of additional dielectric to reduce the size of the ferrite element and associated matching structures.

7. Experimental methods.

Where accurate measurement of phase is to be performed in the presence of appreciable mismatches, we have used a circuit capable of yielding a complete characterization of the scattering coefficients. The bridge-like circuit used for these measurements is shown schematically in Fig. 13B. The output of the signal generator is split into two mutually isolated arms and fed through the test specimen from opposite directions. The circuit includes attenuators and a mechanical phase shifter for adjusting the amplitudes and relative phase of the two signals. The standing wave resulting from scattering by the specimen is observed by means of a slotted section, detector, and oscilloscope or null-detecting meter.

Assuming that the specimen is reciprocal and symmetrical, let R and S denote respectively its complex reflection and transmission coefficients defined at a convenient reference plane. Denote by r the (real) ratio of amplitudes of the two incident signals and by φ their relative phase. With a signal of unit amplitude incident on the specimen from the left in the diagram, a wave R is reflected and returns to the slotted section. Also, a wave $re^{i\varphi}$ is incident from the right, emerging on the left side of the specimen as $Sre^{i\varphi}$. The sum of these two waves constitutes an apparent net "reflection" whose phase Ψ can be observed by adjusting the attenuators so as to produce an infinite VSWR in the slotted section and observing the position of the

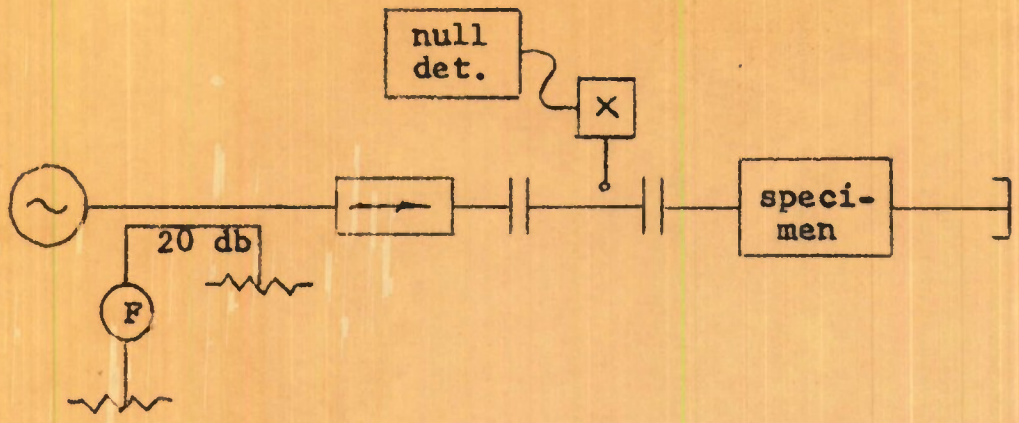

Fig. 13A. Circuit for transmission phase measurement.

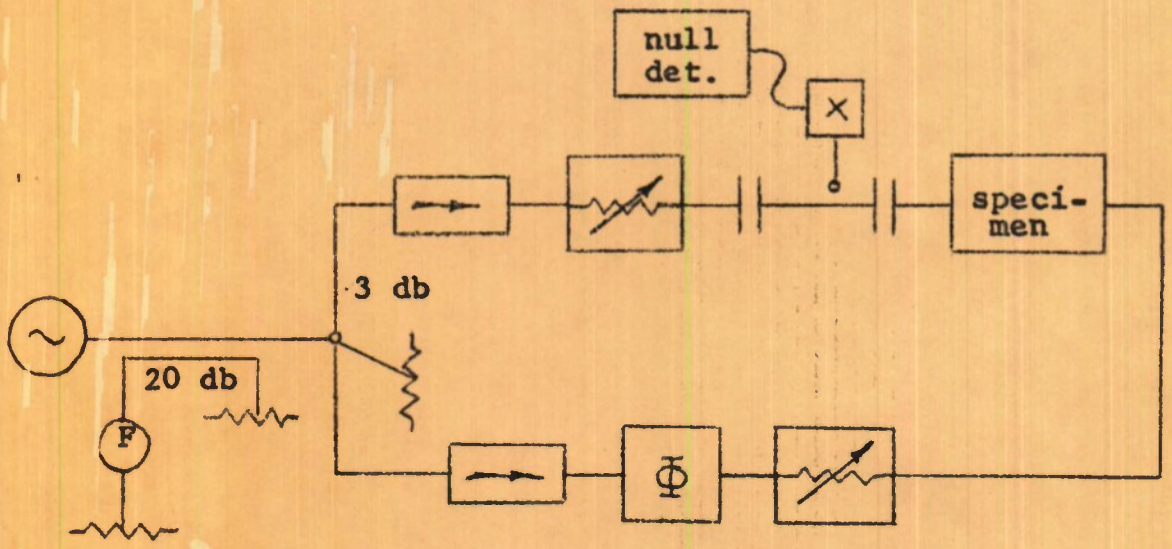

Fig. 13B. Circuit for scattering coefficient measurement.

standing-wave null. The net "reflection" then satisfies

$$R + Sre^{i\varphi} = e^{i\psi} \qquad (42)$$

Equation (42) may be illustrated graphically as shown in Fig. 14 in which the point on the unit circle represents $e^{i\psi}$, shown as the sum of R and $Sre^{i\varphi}$.

By observation of the attenuator readings and position of the null, repeated at each of a number of settings of the variable phase shifter (indicated by Φ in Fig. 13B), it is possible to construct a "best fit" to the diagram of Fig. 14, which exhibits the complex reflection and transmission coefficients and also indicates the dissipative losses. For measurements on the rotating field phaser, the process is repeated at each of a series of orientations of the magnet. The resulting data can be presented as a sequence of vectors in the reflection coefficient plane. Fig. 15 shows an example of such a sequence, together with a tabulation of the magnitudes of R and S and of the transmitted power $\alpha^2 = |R|^2 + |S|^2$ in a particular case.

For work in which less precision is required and in which speed and flexibility in frequency, mechanical structure, etc., are more important, a simpler method was used. The circuit is shown in Fig. 13A. A shorting plate was placed at the output end of the device, and the phase change in two traversals was observed by measuring the position of a standing-wave minimum at the input end. The method is quite satisfactory if the device is well matched; its primary weakness in that case is that the VSWR is degraded because

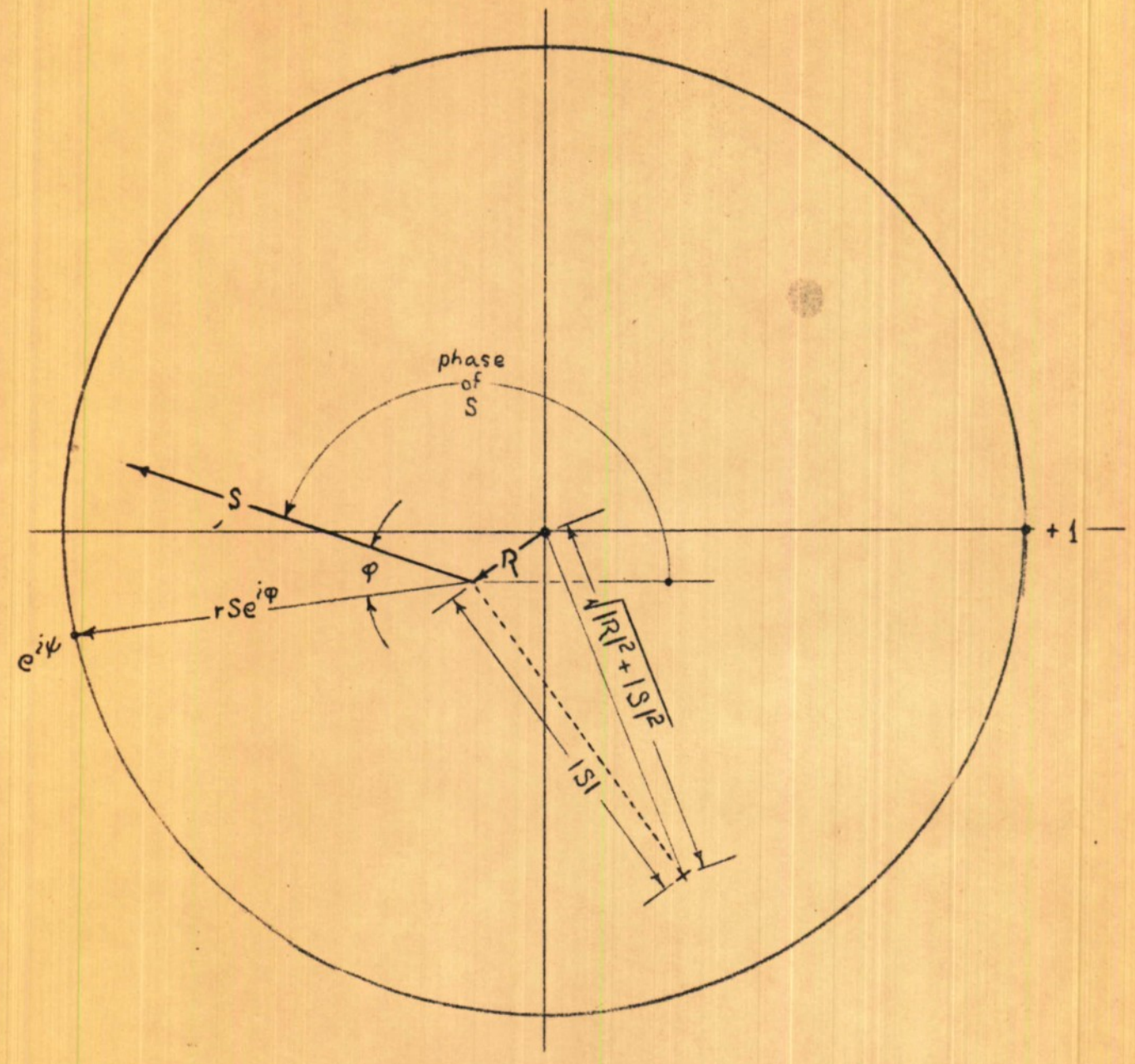

Fig.14. Key to scattering coefficient diagram.

ϑ	$\lvert R \rvert$	$\lvert S \rvert$	phase of S	α	α^2, db
0	0.182	0.691	350°	0.715	2.92
30	242	671	60	713	2.93
60	215	701	110	733	2.69
90	180	758	161	779	2.17
120	143	764	216	777	2.19
150	096	719	273	725	2.79
180	189	686	338	711	2.95

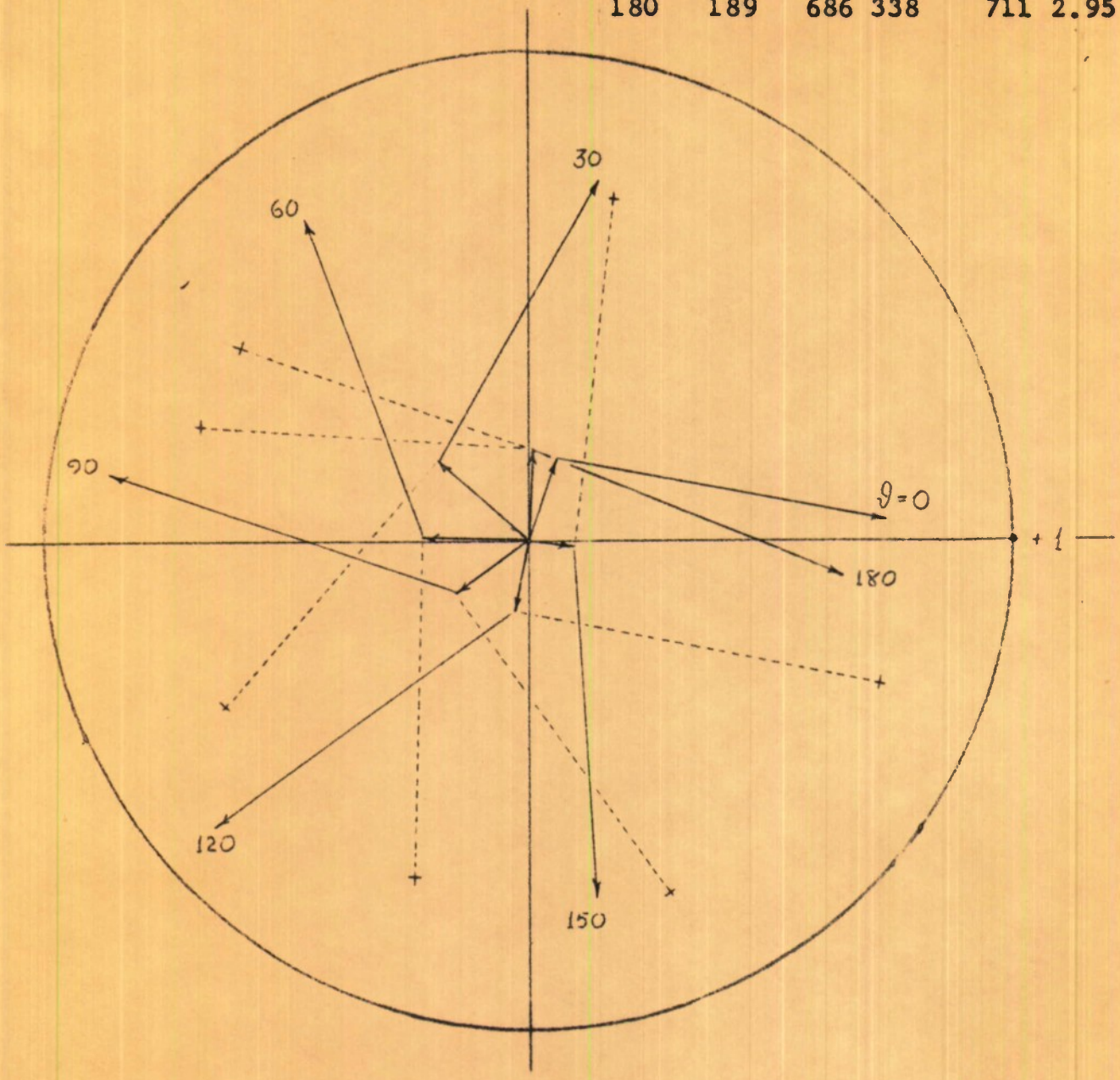

Fig. 15. Illustrating the scattering-coefficient diagram of the rotating-field phaser.

of attenuation in the device, yielding some uncertainty in the position of the minimum. In the presence of mismatches, however, it measures only the net effect of the mismatches separated by a variable electrical length introduced by the phaser itself; it is this error which is included in the data of Fig. 6 and referred to in the associated text.

8. Conclusions

To summarize the results of this program of development on the rotating-field phaser: a ferrite differential half-wave section has been developed which demonstrates the feasibility of performing this function with dielectric, rather than conductive, waveguide propagation. This design is potentially capable of offering extremely high speed in digital or continuous phase variation. Some essential characteristics of the phaser principle, namely the correlation between phase angle and orientation of the control field, unlimited monotonic phase variation, and low insertion loss, have been observed and studied. The design exhibits the features of compactness and structural simplicity inherent in this device.

Although broadband operation was not observed directly, study of bandwidth problems has led to considerable progress, both theoretical and experimental, in determining the conditions for satisfactory dielectric-waveguide performance, developing techniques for matching, and identifying the sources of the disturbances which limit bandwidth and distort phase. Specifically, spurious scattering in the quarter-wave transducers in combination with mismatches at the ferrite half-wave section have been shown to be capable of producing disturbances having the observed features and magnitude. The program has yielded insight into these problems which we believe provides the means for elimi-

nating them.

Because an unexpectedly large part of the effort was required to study and improve the transmission conditions cited above, less attention could be devoted to problems associated with the objective of low-field operation within the period of the program. With the improvement achieved so far it would be possible to observe directly the relation between ferrite composition and tube geometry on the one hand and d-c field dependence of phase and scattering on the other. On the basis of our experience with this and other ferrite devices we believe that this objective can be fulfilled as originally envisioned. Investigation of hysteresis effects has shown that no practical limitations in performance from this source are present. Temperature-sensitivity appears from preliminary measurements to be quite small, although the obscuring effects of transmission disturbances prevented us from evaluating temperature effects to our satisfaction.

Study of the possibility of adapting the design for L-band frequencies has shown that the primary limitation is one of finding a suitable ferromagnetic material. Only one type of material, a chemically substituted version of yttrium-iron garnet, appears available at present to fulfill the requirements of this device, especially that of low insertion loss. Unfortunately its cost is more than double that of most ferrites. Aside from this limitation, the techniques and principles we have learned from the study

program at X-band are applicable to an L-band version.

Progress within the scope of this program has indicated that use of the ferrite rotating-field phaser in phase-array and other applications is a practical possibility. The most serious limitations have been examined and analyzed, and it appears that they can be removed without departing materially from the design as originally conceived.

References

		page
1.	A.G. Fox: An Adjustable Waveguide Phase Changer; Proc. IRE 35 1489-1498 (Dec., 1947).	4
2.	D.H. Ring: A Microwave Double-Detection Measuring System with a Single Oscillator; presented at the High-Frequency Measurements Conference, Jan., 1953.	5
3.	M.T. Weiss and A.G. Fox: Magnetic Double Refraction at Microwave Frequencies; Phys. Rev. 88 146-147 (Oct. 1, 1952).	5,8,13
4.	John C. Cacheris: Microwave Single-Sideband Modulator Using Ferrites; Proc. IRE 42 1242-1247 (Aug., 1954).	5,8,13, 15,16
5.	N. Karayianis and J.C. Cacheris: Birefringence of Ferrites in Circular Waveguide; Proc. IRE 44 1414-1421 (Oct., 1956).	5,15
6.	W.M. Elsasser: Attenuation in a Dielectric Circular Rod; J. Appl. Phys. 20 1193-1196 (Dec., 1949).	7
7.	C.E. Barnes: Broad-Band Isolators and Variable Attenuators for Millimeter Wavelengths; IRE Trans. PGMTT 9 519-523 (Nov., 1961).	7
8.	P. Mallach: Untersuchungen an dielektrischen Wellenleitern in Stab- und Rohrform; Fernmeldetechnische Zeits. (FTZ) 8 8-13 (Jan., 1955).	8,16,20
9.	D. Polder: On the Theory of Ferromagnetic Resonance; Phil. Mag. 40 99-115 (Jan., 1949).	9,13
10.	F. Reggia and E.G. Spencer: A New Technique in Ferrite Phase Shifting for Beam Scanning of Microwave Antennas; Proc. IRE 45 1510-1517 (Nov., 1957).	9,53
11.	J.A. Weiss: A Phenomenological Theory of the Reggia-Spencer Phase Shifter; Proc. IRE 47 1130-1137 (June, 1959).	9,22,53
12.	R.C. LeCraw and E.G. Spencer: Domain Structure Effects in Anamalous Ferrimagnetic Resonance of Ferrites; J. Appl. Phys. 28 399-405 (April, 1957).	21,52
13.	J.A. Weiss: An Interference Effect Associated with Faraday Rotation, and its Application to Microwave Switching; Proc. AIEE Conference on Magnetism and Magnetic Materials, Boston, Oct., 1956; pp. 580-585.	33,48
14.	R.D. Tompkins: A Dispersionless Dielectric Quarter-Wave Plate in Circular Waveguide; Proc. IRE 48 1171-1172 (June, 1960). R.D. Tompkins: A Broad-Band Dual-Mode Circular Waveguide Transducer; IRE Trans. PGMTT 4 181-183 (July, 1956).	35,56

Figures